京都大学
KYOTO UNIVERSITY

Title	Protease homolog BepA (YfgC) promotes assembly and degradation of -barrel membrane proteins in Escherichia coli
Author(s)	Narita, Shin-Ichiro; Masui, Chigusa; Suzuki, Takehiro; Dohmae, Naoshi; Akiyama, Yoshinori
Citation	Proceedings of the National Academy of Sciences of the United States of America (2013)
Issue Date	2013-09-03
URL	http://hdl.handle.net/2433/178690
Right	©2013 by the National Academy of Sciences
Type	Journal Article
Textversion	author

Classification: BIOLOGICAL SCIENCES, Cell biology

Protease homolog BepA (YfgC) promotes assembly and degradation of β-barrel membrane proteins in *Escherichia col*i

Short title: Quality control of β-barrel proteins by BepA

Shin-ichiro Narita[a,b], Chigusa Masui[a], Takehiro Suzuki[c], Naoshi Dohmae[c], and Yoshinori Akiyama[a,1]

[a]Institute for Virus Research, Kyoto University, Kyoto 606-8507, Japan; [b]Faculty of Nutritional Sciences, The University of Morioka, Takizawa, Iwate 020-0183, Japan; and [c]Global Research Cluster, RIKEN, Saitama 351-0198, Japan

[1]To whom correspondence should be addressed:

Yoshinori Akiyama

Institute for Virus Research, Kyoto University, Kyoto 606-8507, Japan

E-mail yakiyama@virus.kyoto-u.ac.jp

Abstract

Gram-negative bacteria are equipped with quality control systems for the outer membrane (OM) that sense and cope with defective biogenesis of its components. Accumulation of misfolded outer membrane proteins (OMPs) in *Escherichia coli* leads to activation of σ^E, an essential alternative σ factor that upregulates transcription of multiple genes required to preserve OM structure and function. Disruption of *bepA* (formerly *yfgC*), a σ^E-regulated gene encoding a putative periplasmic metalloprotease, sensitizes cells to multiple drugs, suggesting that it may be involved in maintaining OM integrity. However, the specific function of BepA remains unclear. Here, we show that BepA enhances biogenesis of LptD, an essential OMP involved in OM transport and assembly of lipopolysaccharide, by promoting rearrangement of intramolecular disulfide bonds of LptD. In addition, BepA possesses protease activity and is responsible for the degradation of incorrectly folded LptD. In the absence of periplasmic chaperone SurA, BepA also promotes degradation of BamA, the central OMP subunit of the β-barrel assembly machinery (BAM) complex. Interestingly, defective oxidative folding of LptD caused by *bepA* disruption was partially suppressed by expression of protease-active site mutants of BepA, suggesting that BepA functions independently of its protease activity. We also show that BepA has genetic and physical interaction with components of the BAM complex. These findings raised the possibility that BepA maintains the integrity of OM both by promoting assembly of OMPs and by proteolytically eliminating OMPs when their correct assembly was compromised.

Significance Statement

Outer membrane proteins (OMPs) are involved in important cellular activities in gram-negative bacteria. Although the *bepA* (formerly *yfgC*) gene encoding a putative metalloprotease has been implicated in quality control of OMPs, its specific function remains unclear. This study reveals that BepA promotes assembly of LptD, an OMP involved in the transport of lipopolysaccharides, which undergoes intramolecular disulfide rearrangement during its biogenesis. BepA also promotes degradation of incorrectly folded LptD. BamA, another OMP involved in OMP assembly, is also degraded in a BepA-dependent manner in the absence of periplasmic chaperone SurA. BepA thus controls the quality of OMPs by promoting either the biogenesis or elimination of OMPs, depending on their folding state.

/body

The cell envelope of gram-negative bacteria is composed of two layers of biological membranes, the outer membrane (OM) and the inner (cytoplasmic) membrane (IM); the periplasmic space that separates these membranes contains a thin layer of peptidoglycans. Outer membrane proteins (OMPs) span the OM with amphipathic, antiparallel β-strands that form a barrel structure. OMPs are synthesized in the cytoplasm with a cleavable signal peptide at their N-termini and are translocated across the IM through the Sec translocon (1). Signal peptide-processed OMPs are transported across the periplasmic space with the aid of periplasmic chaperones, such as SurA, Skp, and DegP, and are inserted into the OM through the function of the β-barrel assembly machinery (BAM) complex (2). The BAM complex is composed of five components: BamA, an essential OMP belonging to the Omp85 superfamily that includes the mitochondrial Sam50 and chloroplast Toc75 proteins, and four lipoprotein subunits (BamB-E) (3-6). BamD is essential for the growth of *Escherichia coli*, while the other three lipoprotein subunits are dispensable (5-7). BamA contains periplasmically exposed polypeptide transport-associated (POTRA) domains that bind the lipoprotein subunits of the BAM complex as well as substrate OMPs (8).

LptD, another essential OMP of gram-negative bacteria, is involved in the assembly of lipopolysaccharide (LPS), a major OM constituent, in the OM (9). LPS is essential for the function of the OM as a permeability barrier. It is synthesized in the IM and targeted to the outer leaflet of the OM through the functions of seven Lpt proteins (LptA–G). LptBFGC and LptDE constitute IM and OM complexes, respectively, and LptA connects these two complexes by shuttling or forming a bridge between the two membranes (10-14). While LptD is involved in flipping of LPS from the periplasmic side to the outer side of the OM (9), LptE is thought to contribute to LPS transport through promotion of LptD folding (15). However, a recent view by

4

Kahne and colleagues suggested that LptE also directly contributes to LPS transport by serving as a "plug" for the lumenal pore of LptD and by acting as a part of the OM LPS translocon together with LptD (16, 17). LptD has two intramolecular disulfide bonds and requires DsbA, a periplasmic oxidoreductase, for its oxidative folding (18, 19). Recently, Chng et al. reported that LptD is assembled into the OM via formation of a folding intermediate containing non-native disulfide bonds that are finally isomerized to native disulfide bonds (17). Importantly, folding of the LptD β-barrel is rate-limiting for maturation of LptD and precedes disulfide isomerization, the step triggered by association with LptE. Analysis with a DsbA mutant that forms kinetically stable mixed-disulfide intermediates with substrates suggested that DsbA is involved in formation of both non-native and native disulfide bonds in LptD (17). A previous study also suggested that DsbC participates in the oxidative folding of LptD (17, 20), although disruption of the *dsbC* gene had little effect on the stability of LptD (19).

Consistent with the vital roles of the cell envelope, *E. coli* is equipped with multiple envelope stress response systems to sense and cope with disorders of OM constituents (21). Among them, the σ^E-dependent stress response system is the only essential one and is probably one of the most important for the maintenance of the OM structure and function. Imbalanced biogenesis and/or defective assembly of OMPs and LPS leads to cytoplasmic activation of σ^E, an extracytoplasmic function σ factor responsible for the transcription of a class of genes involved in biogenesis and quality control of the OM components, including those for subunits of the BAM complex and LPS biosynthetic enzymes (22-24).

To date, 114 genes have been identified as members of the *E. coli* σ^E regulon (24); however, their functions are not fully understood, making them a treasure trove for identification of novel regulators of OM integrity. The products of the σ^E-controlled genes included four periplasmic protease homologs, DegP, PtrA, YhiJ, and YfgC. DegP is a

protease/chaperone that can switch between these activities, thereby acting in both the assembly and elimination of OMPs (25-27). In contrast, functions of the other three protease homologs remain largely unknown. Recently, genome-wide comprehensive analyses of the antibiotic sensitivity of an *E. coli* single-gene knockout library showed that disruption of the *yfgC* gene renders cells sensitive to multiple drugs (28-31). Moreover, profiling of the chemical sensitivities of Δ*yfgC* cells has suggested that this putative protease is involved in the biogenesis and/or quality control of OMPs (31). The amino acid sequence of YfgC indicates that it belongs to the peptidase M48 family and possesses a typical zinc metalloproteinase active site motif, $H^{136}EXXH$. In addition, the C-terminal portion of YfgC contains 4 copies of the tetratricopeptide repeat (TPR) motif, a structural element involved in protein-protein interactions (32). Members of the M48 family include mitochondrial Oma1 (33), Ste24p (34), and *E. coli* HtpX (35). HtpX is a membrane-anchored protease with its protease-active site exposed to the cytoplasm and is thought to collaborate with the AAA^+ protease FtsH to eliminate misfolded IM proteins (36). YfgC has recently been reported to interact with and contribute to proper localization of LoiP (YggG), an OM-associated protease homologous to YfgC (37). However, the proteolytic activity of YfgC has not been demonstrated, and its specific cellular function remains obscure.

In this study, we sought to determine the molecular functions of YfgC in maintaining the structure and function of the cell envelope. Our results suggest that YfgC exerts dual functions, promoting either the biogenesis or proteolytic elimination of OMPs, depending on the folding state of the OMPs. Therefore, we suggest that YfgC should be renamed as BepA (*β*-barrel assembly-*e*nhancing *p*rotease).

Results

BepA processes a protease activity that is important for maintenance of the OM integrity.

While BepA carries a conserved zinc metalloprotease active site motif, $H^{136}EXXH$, it is not known whether BepA possesses a protease activity. To verify whether BepA is indeed a protease, we purified C-terminally decahistidine (His_{10})-tagged wild-type BepA ($BepA_{His10}$) and its derivative with an amino-acid substitution (E137Q) in the metalloprotease active site motif by metal affinity chromatography. Incubation of α-casein, a model substrate, with wild-type $BepA_{His10}$ gave rise to a small but significant amount of a band that migrated slightly faster than α-casein (Fig. 1*A*, open arrowhead). The N-terminal sequence of this band turned out to be FVAPF that matches the 24th to 28th residues of α-casein, indicating that it was generated by cleavage between F^{23}-F^{24}. Generation of this fragment was inhibited when metal chelating reagent 1,10-phenanthroline or EDTA was included in the reaction mixture (Fig. 1*B*). Furthermore, incubation of α-casein with the protease active site motif mutant, $BepA(E137Q)_{His10}$, did not produce such a fragment (Fig. 1*A*). Although the observed *in vitro* proteolytic activity of BepA is rather low for unknown reasons, the above results collectively demonstrate that BepA is indeed a metalloprotease.

Disruption of the *bepA* gene causes significantly elevated sensitivity to high-molecular mass antibiotics, such as erythromycin and vancomycin (28-31; Fig. 1*C*), indicating that loss of BepA compromises the function of OM as a permeability barrier. We examined the complementation activities of two active site motif mutants, BepA(E137Q) and BepA(H136R), against the Δ*bepA* mutation. In contrast to wild-type BepA, these mutants failed to restore drug resistance to the Δ*bepA* mutant (Fig. 1*C*), although they accumulated at levels comparable to the wild-type protein (Fig. 1*D*). Importantly, these protease-dead mutants exhibited a

dominant-negative phenotype, as their expression in the wild-type (*bepA*⁺) strain significantly

increased sensitivity to erythromycin (Fig. 1*C*). It is not unexpected that proteases with a

compromised proteolytic active site can exhibit a dominant-negative phenotype since they often

retain other activities (e.g., substrate binding, oligomerization) and thus compete with the

wild-type protein. These results suggest that protease activity of BepA is important for its

function to maintain OM integrity. Indeed, as described in later sections (see Fig. 5 and 8), our

results demonstrate that BepA is involved in degradation of misfolded OMPs.

Isolation of multicopy suppressors of the *bepA*-null mutation. Despite apparent dysfunction

of OM, disruption of *bepA* gene has little impact on the profiles of OMPs and heat modifiability

of a major OMP, OmpA (Fig. S1). To gain insight into the role of BepA in the envelope

function, we sought multicopy suppressors of the Δ*bepA* mutation. Multicopy suppressors

provide clues to important functions of a deleted gene by identifying alternative routes to

performing the key function disabled by the gene deletion. While the Δ*bepA* strain was sensitive

to erythromycin, the Δ*bamE*/Δ*bepA* strain showed greater sensitivity to multiple drugs than the

bepA deletion alone (see Fig. 6*A* and *B*). We thus used the double-mutant strain as the basis for

the multicopy suppressor screen. For this screen, we used the ASKA clone library of 4,123 *E.*

coli open reading frames (ORFs), individually cloned under the isopropyl-thio-β-D

-galactopyranoside (IPTG) -inducible promoter of a chloramphenicol-resistant multicopy vector

(38). Pools of ASKA clones were introduced into the Δ*bamE*/Δ*bepA* strain, and transformants

were selected on agar plates containing 20 μg/mL chloramphenicol and 5 μg/mL erythromycin,

with (100 μM) or without IPTG to induce the cloned genes. Both regimes were utilized because

high expression can sometimes be toxic. Among the ASKA pools, we found 9

erythromycin-resistant transformants without IPTG, and 248 transformants with IPTG. After

verifying that drug resistance was linked to each plasmid (by retransformation with plasmids

isolated from the first isolated drug-resistant bacteria), cloned genes were identified by DNA sequencing. We then tested whether these multicopy suppressors conferred resistance to other $\Delta bamE$/$\Delta bepA$-derived drug sensitivities (e.g., SDS and vancomycin; Table S1) and retained the 14 clones that conferred resistance to all of the selection reagents. Of these, only the clone carrying *lptE* conferred erythromycin and vancomycin resistance to a level comparable to a plasmid carrying wild-type *bepA*, even in the absence of IPTG (Fig. 2*A* and Table S1). Furthermore, when *lptE* was under tight arabinose control, the erythromycin sensitivity of the $\Delta bepA$ strain was suppressed in an arabinose-dependent manner (Fig. 2*B*). These results established that overexpression of LptE compensated for the lack of BepA, at least with respect to the drug-sensitive phenotypes examined. LptE/D form the essential OM translocon that is required for export of LPS to the outer leaflet of the OM (9, 10, 16), and LptE assists the biogenesis and/or function of LptD (10, 15-17), suggesting that BepA may participate in the formation of functional LptD.

LptD with non-native disulfide bonds accumulates in the absence of BepA. LptE promotes the proper oxidation of LptD and stabilizes LptD protein (19, 39). It seemed thus possible that lack of BepA, like that of LptE, destabilizes LptD. Also, considering that drug sensitivity of the $\Delta bepA$ strain was suppressed by overproduction of LptE, it might be also possible that the *bepA* disruption might cause decrease in the LptE level. However, these were ruled out, as the levels of LptD and LptE were little affected by the presence or absence of BepA (Fig. 3*A*, + ME). We next considered whether BepA affected disulfide bond formation in LptD. Mature LptD has two intramolecular disulfide bonds between nonconsecutive pairs of Cys residues (C_{31}-C_{724} and C_{173}-C_{725}; mature LptD with correct disulfide bonds referred to here as LptD^{NC}) (19). As reported previously (19), correctly disulfide-bonded LptD^{NC} migrates more slowly than the fully reduced form (Fig. 3*A*, - ME, left lane). Importantly, the $\Delta bepA$ strain had an additional band

9

(LptD^C) that migrated more rapidly than the fully reduced band (Fig. 3A, - ME, right lane).

To unambiguously establish that different disulfide bond connectivity was responsible for generation of LptD^C, we examined the migration patterns of C-terminally hexahistidine (His$_6$)-tagged LptD proteins (LptD$_{His6}$) having various combinations of their four Cys residues changed to Ser, thereby restricting which disulfide bonds were able to form. LptD(CCSS)$_{His6}$, which formed only the sequential C$_{31}$-C$_{173}$ disulfide bond, gave only the rapidly migrating species, even in the wild-type ($bepA^+$) strain (Fig. S2A). In contrast, LptD(SSCC)$_{His6}$, which formed only the sequential C$_{724}$-C$_{725}$ disulfide-bond, did not produce this rapidly migrating species. As reported (17), the C$_{724}$-C$_{725}$ disulfide bond can actually be formed, as this species was nonreactive with the sulfhydryl-reactive alkylating reagent, maleimide PEG$_2$-biotin, unless it had been reduced with DTT before the alkylating reaction (Fig. S2B). All species that could form the C$_{31}$-C$_{173}$ bond (CCCC, CCSC, and CCCS) promoted LptD^C formation in the absence of BepA (Fig. S2A). We thus concluded that LptD^C had non-native disulfide bonds, at least between C$_{31}$ and C$_{173}$ and possibly between C$_{724}$ and C$_{725}$ (Fig. 3B). Subcellular fractionation revealed that, like LptD^{NC}, LptD^C was associated with the OM (Fig. S2C and D).

BepA promotes formation of the proper intramolecular disulfide bonds in LptD. It has been recently reported that LptD is assembled into the OM via formation of an intermediate containing non-native disulfide bonds linked between consecutive Cys residues that are isomerized to native disulfide bonds, the step triggered by assembly with LptE (17). Our results suggest that LptD^C corresponds to the folding intermediate with consecutive disulfide bonds and the absence of BepA causes its accumulation. To determine whether LptD^C is indeed an on-pathway species, we examined the kinetics of formation of LptD^{NC} and LptD^C by pulse-labeling cells with [^{35}S]-methionine for 1 min, followed by chase with excess non-labeled methionine. In wild-type cells, almost all labeled LptD molecules were present as LptD^C after a

1-min chase and were then converted to LptD^{NC} in a process in which an initial rapid ($t_{1/2}$ ~10 min) phase was followed by a slower conversion that took approximately 40 min for completion (Fig. 4A). Like in wild-type cells, LptD was mostly detected as LptD^C after a 1-min chase in $\Delta bepA$ cells and was converted to LptD^{NC} upon chase. However, this conversion took a much longer time ($t_{1/2} > 80$ min; Fig. 4A) in $\Delta bepA$ cells. Conversely, the rate of LptD^C to LptD^{NC} conversion was restored by overproduction of BepA in $\Delta bepA$ cells (Fig. 4B). The conversion was slightly but significantly accelerated by overproduction of BepA, even in wild-type cells (Fig. S3). These results indicate that BepA promotes disulfide isomerization of LptD and that the process promoted by BepA is rate-limiting for LptD maturation. Importantly, overexpression of LptE in $\Delta bepA$ cells promoted both the extent and rate of the conversion of LptD to approximately those of wild-type cells (Fig. S4), suggesting that the suppression of $\Delta bepA$ by LptE overexpression resulted mainly from restoration of LptD^{NC} formation.

We found that ectopic expression of the H136R or E137Q mutant of BepA in $\Delta bepA$ cells also promoted LptD^C to LptD^{NC} conversion, albeit less effectively than wild-type BepA (Fig. 4B). In contrast, these mutants slightly retarded this conversion process when expressed in wild-type ($bepA^+$) cells (Fig. S3), which was consistent with their dominant-negative properties. These results indicated that BepA could promote oxidative folding of LptD independently of its protease activity, although the intact protease motif is still required for its full functioning.

Disulfide isomerization of periplasmic and OM proteins is mainly catalyzed by DsbC (18), but that of LptD proceeds even in the absence of DsbC (17; Fig. S5A). Additional disruption of the $dsbG$ gene, encoding possible periplasmic disulfide isomerase, had essentially no effect (Fig. S5A). Therefore, DsbC and DsbG may be dispensable for disulfide exchange in the process of LptD biogenesis. The oxidoreductase DsbA is required for the oxidative folding of LptD (17, 18). In the absence of DsbA, several bands, including both LptD^C and LptD^{NC},

were generated after a 1-min chase (Fig. S5*B*). When treated with a reducing reagent, they were converted to LptD^{RED} (Fig. S5*B*), indicating that they were LptD species with different oxidative states. These results suggested that, in the absence of DsbA, both consecutive and nonconsecutive disulfide bonds were formed stochastically.

BepA degrades LptD when LptD fails to form the OM LPS translocon. In agreement with the recent reports by Chng et al. (17), we found that the LptD^C to LptD^{NC} conversion was almost completely blocked in LptE-depleted cells (Fig. 5*A*). In addition, the pulse-chase experiment revealed that LptD^C was significantly destabilized in this condition (Fig. 5*A*). Strikingly, LptD^C became stable, even under LptE-limiting conditions, when *bepA* was disrupted (Fig. 5*A*), and the LptD^C-stabilizing effect of Δ*bepA* was suppressed by expression of wild-type but not protease-dead BepA protein from a plasmid (Fig. 5*B*). Furthermore, ectopic expression of wild-type BepA led to increased destabilization of LptD^C in LptE-depleted cells carrying chromosomal *bepA$^+$*, whereas that of protease-dead BepA mutants dominantly stabilized LptD^C (Fig. 5*C*). These results strongly suggest that BepA functions as a protease *in vivo* to degrade LptD that has failed to interact with LptE to form the functional LPS translocon.

Genetic interaction of *bepA* with *bamB* and *bamE*. The Δ*bepA* strain exhibits elevated drug sensitivity (28-31; Fig. 1*C*), a phenotype reminiscent of deletion of some of the nonessential members (*bamB*, *bamC*, and *bamE*) of the BAM complex (31). The BAM complex, composed of one β-barreled subunit (BamA) and four lipoprotein subunits (BamB–E), facilitates insertion of β-barrel proteins into the OM. The similarities in the antibiotic sensitivity phenotypes of these proteins suggested that BepA may have some functional interaction with the Bam components. Consistent with this idea, Δ*bamB/*Δ*bepA* or Δ*bamE/*Δ*bepA* double mutants displayed elevated sensitivity toward multiple antibiotics (Fig. 6*A*). These double mutants also

exhibited significantly higher SDS sensitivity; they grew much more slowly than the wild-type cells in the presence of 0.5% SDS, although the viability of cells seemed almost the same (Fig. 6*B*). None of the single mutations conferred these phenotypes (Fig. 6*B*). These results show that *bepA* genetically interacts with *bamB* and *bamE*. Interestingly, the protease-dead BepA mutant proteins restored the SDS resistance of the Δ*bamB*/Δ*bepA* strain at 30°C, supporting the above notion that BepA plays a nonproteolytic role (Fig. 6*C*), while they failed to restore the SDS sensitivity of the Δ*bamE*/Δ*bepA* strain. Moreover, these mutant proteins dominantly sensitized the Δ*bamE*/Δ*bepA* cells to SDS at 37°C, underscoring the fact that the residual activity of protease-defective proteins could be deleterious to the cell (Fig. 6*C*).

BepA is localized in close proximity to the BAM complex. We then investigated possible physical interaction with envelope components, such as the BAM complex. The SOSUI program (40) predicted BepA to be a periplasmic protein with an N-terminal 27 amino acid-long signal peptide. As expected, upon cell fractionation, BepA was predominantly recovered in the soluble fraction (Fig. S6). However, a significant amount of BepA was also present in the membrane fraction (Fig. S6). As an unbiased approach to identify putative BepA binding partners, we used chemical cross-linking. Wild-type cells with a plasmid encoding C-terminally His$_{10}$-tagged BepA (BepA$_{His10}$) or its H136R or E137Q derivatives were converted to spheroplasts and treated with bis(sulfosuccinimidyl) suberate (BS^3), a membrane-impermeable and amine-reactive cross-linker, and analyzed by SDS-PAGE and anti-BepA immunoblotting (Fig. 7*A*). BepA$_{His10}$ gave rise to several cross-linked products (Fig. 7*A*), which were even more obvious with BepA(H136R)$_{His10}$ and BepA(E137Q)$_{His10}$. Enhanced cross-linking with protease-dead mutants may be attributable to stalling reactions caused by impaired protease activity. Metal affinity chromatography followed by liquid chromatography-mass spectrometry analysis of the strongest cross-linked band of

BepA(E137Q)$_{His10}$ (~170 kDa) identified BamA, the central subunit of the BAM complex (Fig. S7). Immunoblotting with anti-BamA antibodies confirmed BamA-BepA cross-linking (Fig. 7B). As expected, BamA-BepA adducts were almost exclusively recovered in the membrane fraction (Fig. 7B). To examine the possible interaction of BepA with other subunits of the BAM complex, we compared the patterns of BS^3-mediated adduct production in the presence or absence of the nonessential lipoprotein subunits, i.e., BamB, BamC, or BamE. In addition to the BamA-BepA(E137Q) adduct detected in all strains (Fig. 7C and D), a cross-linked product of ~110 kDa, reactive with both anti-BepA and anti-BamC antisera, was detected in wild-type, Δ*bamB*, and Δ*bamE* strains, but not in the Δ*bamC* strain (Fig. 7C and F). Additionally, an ~85-kDa band reactive with both anti-BepA and anti-BamD antisera was detected in the Δ*bamC* strain (Fig. 7C and G). No cross-link between BepA and BamB was observed (Fig. 7E).

As an alternative approach to probe possible interaction, we carried out site-directed *in vivo* cross-linking experiments. The C-terminal portion of BepA contains four copies of the TPR motif, which is widely involved in protein-protein interactions. We expected that the BepA TPR motifs would participate in interaction with other proteins and substituted an amber codon for the Q428 codon in the fourth TPR motif of BepA, to allow suppressor tRNA-mediated introduction of a non-natural, photo-reactive amino acid, *p*-benzoylphenylalanine (pBPA), at this position (41). Cells expressing BepA(Q428pBPA) were UV-irradiated and analyzed by SDS-PAGE and immunoblotting. We found that a band of about 135 kDa that was reactive with both anti-BepA and anti-BamA antibodies was yielded in UV-irradiation and pBPA-dependent manners (Fig. 7H), indicating that it represents a BamA-BepA(Q428pBPA) adduct.

The BAM complex is rather stable, enabling purification of the entire BAM complex using a polyhisitidine tag attached to a BAM component (6, 42). To examine whether formation of the cross-linked adducts reflects direct interaction between BepA and the BAM complex,

BepA(E137Q) was co-expressed with C-terminally His$_6$-tagged BamB (BamB$_{His6}$) in the $\Delta bamB$ strain. Metal affinity chromatography followed by SDS-PAGE and immunoblotting revealed that, along with other Bam components, a portion of BepA(E137Q) was co-isolated with BamB$_{His6}$ (Fig. 7I). Taken together, these results strongly suggest that BepA directly interact with the BAM complex possibly via its TPR domain. Its membrane localization could be at least partly resulted from this interaction.

BepA cleaves BamA in cells lacking SurA. The above finding that BepA interacts with BamA prompted us to examine the possibility that BamA becomes a proteolytic substrate of BepA. In the wild-type background, however, we detected no difference in the profiles of anti-BamA-reactive bands between wild-type and $\Delta bepA$ strains (Fig. 8, upper panel, lanes 1 and 2). We next compared the profiles of anti-BamA-reactive bands in the $\Delta surA$ background. SurA is thought to play a primary role in the biogenesis of OMPs, and disruption of the $surA$ gene causes massive decreases in the levels of OMPs and increased permeability to a wide variety of drugs (43). Absence of SurA does not affect β-barrel folding of BamA in cells grown in rich media (44). However, we detected several anti-BamA-reactive bands that were smaller than intact BamA in $\Delta surA$ cells when the cells were grown in minimal media. These bands were hardly detected in $\Delta surA/\Delta bepA$ double mutants (Fig. 8, upper panel, lanes 3 and 4) but regenerated upon ectopic expression of wild-type but not protease-dead BepA proteins (Fig. 8, upper panel, lanes 5–8) in the same strain background, suggesting that they are BamA degradation products. Degradation of other OMPs such as LamB and OmpA was not observed (Fig. S8A and B) under similar conditions. Loss of SurA could induce the σ^E stress response and cause upregulation of BepA. However, BamA degradation observed in the $\Delta surA$ strain was not the direct results of increased synthesis of BepA, because overexpression of BepA in the $surA^+$ strain did not cause BamA degradation (Fig. S8C). It is unclear why BamA degradation

15

products were not detected in cells grown in rich media, but they may be further degraded by other proteases in that case. Collectively, these results suggest that proper assembly of BamA is compromised in the absence of SurA and that BepA degrades BamA under such a condition. Alternatively, as BamA has been suggested to assume different conformations during its functional cycle (45, 46), the absence of SurA might cause accumulation of the BepA-susceptible form of BamA.

We noticed that C-terminally His_{10}-tagged wild-type BepA migrated faster than its H136R or E137Q derivative and migrated slightly slower than chromosomally-encoded BepA upon SDS-PAGE (Fig. 8, lower panel). It seems likely that BepA$_{His10}$ underwent self-cleavage within its C-terminally attached tag sequence, which further supports our result that BepA possesses proteolytic activity.

Discussion

In this study, we investigated the cellular functions of BepA, a σ^E-regulated, periplasmic protease homolog implicated in the maintenance of OM integrity. With a purified preparation, we demonstrated that BepA indeed possesses a proteolytic activity. Our genetic and biochemical analyses suggest that BepA acts in the assembly/degradation of two essential OMPs, LptD and BamA, the central components of OM translocons for LPS and OMPs, respectively. Importantly, we showed that BepA can promote disulfide isomerization of LptD independently of its protease activity and degradation of LptD and BamA when their proper assembly is compromised. Our results suggest that BepA acts as a protease/chaperone that contributes to OM quality control by directly and/or indirectly affecting biogenesis of both OMPs and LPS.

BepA promotes maturation of LptD. LptD is converted into the mature form with nonconsecutive disulfide bonds (LptD^{NC}) via an intermediate with non-native, consecutive disulfide bonds (LptD^C) (17). While Chng et al. identified this intermediate using epitope-tagged LptD expressed from a plasmid (17), we showed that chromosomally encoded LptD also follows this assembly pathway. A detailed study by Kadokura and Beckwith suggested that while disulfide bonds of proteins are formed vectorially from the N-terminus to the C-terminus in the periplasm when the protein is cotranslationally translocated across the IM, post-translationally translocated proteins have more relaxed restrictions for the order of disulfide bond formation (47). Although LptD is presumably exported across the membrane post-translationally, disulfide bonds are exclusively formed in the N-to-C order. The finding that the precursor form of LptD, observed after 1-min chase, migrated more rapidly in nonreducing SDS-PAGE than in reducing gels (Fig. 4*A*) supports that at least the disulfide bond

between C_{31} and C_{173} can be formed before completion of polypeptide translocation. The physical distance between the two Cys pairs (separated by 550 amino acids) may contribute to the exclusive formation of LptD^C, even in a post-translational translocation pathway. DsbA is involved in the oxidative folding pathway of LptD (17-19) and disulfide bonds of LptD are formed stochastically in the absence of DsbA. Oxidants in the media or molecular oxygen may contribute to oxidizing some populations of LptD^{RED} directly to LptD^{NC}, as previously suggested (19), which may be why DsbA is non-essential even though it appears to have critical roles in the biogenesis of essential LptD.

We screened for multicopy suppressors against the drug sensitivity phenotype of the $\Delta bepA$ strain and identified the *lptE* gene that encodes a protein involved in the function and/or folding of LptD (15). This suggests that BepA is also involved in LptD biogenesis. In agreement with this notion, we found that disruption of *bepA* delayed the rearrangement of LptD disulfide bonds, causing accumulation of LptD^C, which was suppressed by overexpression of LptE. Disulfide bond rearrangement in LptD is triggered by its association with LptE (17). Our finding of suppression by LptE overproduction of defective LptD^C-to-LptD^{NC} conversion due to loss of BepA suggests that BepA promotes LptD/E association. Through the isolation and analyses of mutations in *bamA* that allele-specifically suppress an *lptE* mutation, it was proposed that LptE interacts with LptD that is being assembled by the BAM complex (15). BepA may directly assist efficient interaction between LptD and LptE at the BAM complex or act at some other step during LptD assembly to eventually facilitate formation of a productive LptD/E complex (Fig. 9, upper panel).

Possible dual functions of BepA as a chaperone and protease. Here, we purified BepA and showed that it has a low but significant protease activity against α-casein. Its protease activity was inhibited by metal chelating reagents or amino acid substitution in the putative protease

18

active-site motif (HEXXH), suggesting that BepA is a metalloprotease as deduced from its sequence homology to the M48 family of zinc metalloproteinases. Protease-dead BepA mutants are defective in complementation of the $\Delta bepA$ mutation and exert dominant-negative effects when expressed in wild-type ($bepA^+$) cells. Degradation of LptD^C in LptE-depleted cells and BamA in $\Delta surA$ cells was dependent on BepA with an intact protease active-site motif. Moreover, overexpression of wild-type BepA accelerated degradation of LptD^C in LptE-depleted cells, whereas protease-dead BepA mutants dominantly stabilized LptD^C under the same conditions. Our observations collectively suggest that BepA directly proteolyzes OMPs such as LptD and BamA *in vivo* and that protease activity is important for its function in maintaining OM integrity (Fig. 9, lower panel). Although the observed *in vitro* protease activity was quite modest, it might be improved by, for instance, optimization of the assay conditions and/or addition of unidentified partner proteins.

Several lines of evidence suggest that BepA also possesses a protease activity-independent function. We found that the SDS sensitivity of the *bamB/bepA* double disruptant was complemented by protease-dead mutants. Disulfide rearrangement of LptD was also promoted by these protease-dead BepA derivatives. Furthermore, overexpression of BepA in wild-type cells facilitated the rate of LptD^C to LptD^{NC} conversion (Fig. S3) without affecting the stability of LptD. It is thus conceivable that BepA can facilitate formation of the proper conformation of LptD independently of its protease activity. These characteristics of BepA are reminiscent of DegP, another σ^E-regulated protease that reversibly switches between a protease and a chaperone in a temperature- and substrate-dependent manner (25, 27). Our results suggest that BepA is able to function in two ways depending on the folding state of a substrate OMP: as a chaperone promoting the biogenesis of a substrate OMP or as a protease degrading it when it fails to assemble correctly into the OM.

19

It should be noted that rate of LptD^C to LptD^{NC} conversion was not fully restored by the expression of protease-dead BepA mutants in the $\Delta bepA$ strain; the protease-dead mutants effectively recovered the initial rate of LptD^C to LptD^{NC} conversion, but the final yield of LptD^{NC} in protease-dead BepA-expressing cells was much lower than that in the strain expressing wild-type BepA. Although the exact reason for the above observations is unclear, a fraction of LptD^C may elude the protease-dead mutants having reduced or altered chaperon-like activity and enter an off-target pathway after a certain period of time to yield a dead-end product that resists the action of BepA. The protease activity of BepA may also be required for its maximum activity to remove a portion of LptD^C that would misfold, even in the presence of LptE, and competitively inhibit the function of BepA.

BepA is involved in maintenance of OM integrity. *bepA* mutants exhibit hypersensitivity to a variety of hydrophobic and high-molecular-mass drugs. Recent large-scale chemical genomics combined with quantitative fitness measurements have suggested that the function of the *bepA* gene is highly correlated with those of genes involved in OMP and LPS biosynthesis (30, 31). Consistent with the above suggestion, our *in vivo* observation that additional disruption of the *bamB* or *bamE* gene synergistically elevated the SDS and antibiotic sensitivity of the $\Delta bepA$ strain suggested that BepA has genetic interactions with these BAM components and thus is involved in normal OM assembly. Direct interaction between BepA and the BAM complex was suggested from our biochemical results demonstrating that BepA can be pulled down with the BAM complex and cross-linked with BamA, BamC, and BamD. Site-specific *in vivo* photo-crosslinking experiments suggested that the TPR domain of BepA is involved in the interaction with BamA. These observations raise the possibility that BepA acts in cooperation with the BAM complex.

Suppression of the antibiotic hypersensitivity of the $\Delta bepA$ strain by overexpression of

LptE, which would specifically improve the folding/assembly of LptD, suggests that the antibiotic hypersensitivity of this strain is mainly attributable to folding defects in LptD. Inefficient assembly of LptD would result in delay of LPS translocation across the OM, which causes phospholipids to flip from the inner to the outer leaflet of the OM (48). Impaired lipid asymmetry would then abolish the barrier function of OM against drugs. However, BepA may play a more general role in the biogenesis/quality control of OMPs. Synthetic lethal or sick phenotypes are often observed following disruption of two genes that have overlapping or compensatory functions. Indeed, we found that simultaneous disruption of *bepA* together with either *bamB* or *bamE* synthetically sensitized cells to SDS. In addition, BepA can interact with the BAM complex. The genetic and physical interactions between BepA and the BAM complex raise the possibility that BepA promotes the correct assembly of not only LptD but also other OMPs. The *surA/bepA* double disruptant was recently reported to exhibit a temperature-sensitive growth phenotype (49). Lack of SurA would produce misfolded BamA that could be normally eliminated by BepA, and the growth defects of the *surA/bepA* double disruptant may result from dysfunction of the BAM complex to assemble OMPs. Because lack of BepA does not cause a drastic change in β-barrel folding of OMPs that can be assessed by the heat-modifiability assay, it is not easy to assay maturation for most OMPs other than LptD, maturation of which can be assayed by examining the disulfide rearrangement. Improvement of experimental techniques to monitor folding/assembly states of OMPs would be required to test this possibility.

Materials and Methods

Bacterial strains, plasmids, and media. The bacterial strains, plasmids and primers used in this study are listed in Table S2-S4. Their constructions are described in the Supporting Information. *E. coli* K12 strains AD16 (50), MC4100 (51), and AM604 (10) were used as wild-type strains. AM604 and GC187 ($P_{ara}lptE$) were a generous gift from Dr. Thomas J. Silhavy at Princeton University (Princeton, NJ). SM4106 (Δ*bamB*::*tet*) was a generous gift from Dr. Shin-ichi Matsuyama at Rikkyo University (Tokyo, Japan). KRX (Promega) and TOP10 (Invitrogen) were used as hosts for protein expression and routine cloning procedures, respectively. The Keio collection (52), the ASKA library (38), and plasmid pCP20 were provided by the National BioResource Project-*E. coli* (National Institute of Genetics, Mishima, Japan). pEVOL-pBpF was purchased from Addgene (Cambridge, MA). Cells were grown in L medium (containing 10 g/L bactotryptone, 5 g/L yeast extract, and 5 g/L NaCl; the pH was adjusted to 7.2 by NaOH) or M9 medium (53) (with omission of $CaCl_2$), supplemented with ampicillin and chloramphenicol at 50 and 20 μg/mL, respectively, when appropriate.

Selection of multicopy suppressors. A total of 4,123 clones from the ASKA library were divided into 112 groups such that each group contained up to 48 clones. Mixtures of plasmids were prepared from each group and used to transform SN537 (Δ*bepA* Δ*bamE*). Transformants were selected at 30°C on L agar containing 20 μg/mL chloramphenicol and 0 or 5 μg/mL erythromycin in the presence or absence of 100 μM IPTG. Each group yielded 0–14 erythromycin/chloramphenicol-resistant colonies, while 100–300 transformants were obtained on plates containing chloramphenicol but not erythromycin. Plasmids were purified from erythromycin/chloramphenicol-resistant colonies and reintroduced into SN537 to check whether erythromycin resistance was linked to each plasmid. The verified plasmid clones were

sequenced to identify the cloned genes.

Pulse-chase and immunoprecipitation experiments. AD16, GC187, and their derivatives were grown to an early log phase in M9 medium supplemented with 19 amino acids other than methionine, 2 μg/mL thiamine, and 0.2% glucose at 30 or 37°C. Cells carrying a pTH18cr derivative were grown similarly, but in the presence of 0.2% maltose and 1 mM IPTG instead of glucose. Cells were labeled with 370 kBq/mL [^{35}S]-methionine (American Radiolabeled Chemicals) for 1 min at 30 or 37°C, and chase was initiated by the addition of 0.04% (final conc.) nonradioactive methionine. Aliquots were withdrawn after 1, 2, 5, 10, 20, 40, 60, and 80 min, and proteins were precipitated with trichloroacetic acid. Protein precipitates were dissolved in 50 mM Tris-HCl (pH 8.1) containing 1% SDS and 1 mM EDTA, boiled for 5 min, and diluted 20-fold with 50 mM Tris-HCl (pH 8.1) containing 150 mM NaCl, 2% Triton X-100, and 0.1 mM EDTA. After removal of insoluble materials by centrifugation at 20,000 × g for 5 min, the supernatant was subjected to immunoprecipitation with anti-LptD antiserum and Dynabeads Protein A (Invitrogen). Immunoprecipitated proteins were eluted from beads by boiling for 5 min in SDS-PAGE sample buffer with or without 1% 2-mercaptoethanol and were analyzed by SDS-PAGE and phosphorimaging with BAS-1500 (Fujifilm, Tokyo, Japan). Band intensities were quantified with MultiGauge software (Fujifilm).

BS^3-mediated cross-linking. MC4100 derivatives transformed with plasmids that encode BepA derivatives were grown to a late log phase at 30 or 37°C in L medium. Cells were harvested, washed once with buffer A (20 mM sodium-phosphate buffer [pH 7.2] containing 300 mM sucrose), and resuspended in the same buffer. After addition of 40 μg/mL lysozyme, cells were converted to spheroplasts by incubation at 4°C in buffer A containing 1 mM EDTA in the presence or absence of 1 mM BS^3 (Thermo Fisher Scientific) for 30 min. Then, samples were

23

separated into periplasmic and spheroplast fractions by centrifugation at 20,000 × g for 2 min. Spheroplasts were suspended in 50 mM Tris-HCl (pH 7.5) and disrupted by sonication. After removal of unbroken cells by centrifugation at 10,000 × g for 2 min, membranes were collected by ultracentrifugation at 100,000 × g for 30 min. Proteins in the periplasmic and membrane fractions were precipitated by the addition of 10% (final conc.) trichloroacetic acid and were subjected to SDS-PAGE and immunoblotting.

pBPA-mediated photo-crosslinking. SN56 transformed with pUC-BepA(Q428Amber) and pEVOL-pBpF was grown at 30°C to a late log phase in L medium supplemented with 0.2% arabinose and 1 mM IPTG in the presence or absence of 1 mM pBPA (Bachem, Bubendorf, Switzerland). Cells were chilled on ice for 10 min and UV-irradiated at 365 nm on a Petri dish for 10 min by using a B-100AP UV lamp (Ultraviolet Products, Upland, CA) at a distance of 4 cm. Cells were then harvested, suspended in 20 mM Tris-HCl (pH 7.5) and disrupted by sonication. After removal of unbroken cells by centrifugation at 10,000 × g for 2 min, membranes were collected by ultracentrifugation at 100,000 × g for 30 min. Proteins in the membrane fractions were precipitated by trichloroacetic acid and subjected to SDS-PAGE followed by immunoblotting.

References

1. Pugsley AP (1993) The complete general secretory pathway in gram-negative bacteria. *Microbiol Rev* 57(1): 50-108.

2. Ricci DP, Silhavy TJ (2012) The Bam machine: A molecular cooper. *Biochim Biophys Acta* 1818(4): 1067-1084.

3. Voulhoux R, Bos MP, Geurtsen J, Mols M, Tommassen J (2003) Role of a highly conserved bacterial protein in outer membrane protein assembly. *Science* 299(5604): 262-265.

4. Ruiz N, Falcone B, Kahne D, Silhavy TJ (2005) Chemical conditionality: a genetic strategy to probe organelle assembly. *Cell* 121(2): 307-317.

5. Wu T, et al. (2005) Identification of a multicomponent complex required for outer membrane biogenesis in *Escherichia coli*. *Cell* 121(2): 235-245.

6. Sklar JG, et al. (2007) Lipoprotein SmpA is a component of the YaeT complex that assembles outer membrane proteins in *Escherichia coli*. *Proc Natl Acad Sci USA* 104(15): 6400-6405.

7. Malinverni JC, et al. (2006) YfiO stabilizes the YaeT complex and is essential for outer membrane protein assembly in *Escherichia coli*. *Mol Microbiol* 61(1): 151-164.

8. Kim S, et al. (2007) Structure and function of an essential component of the outer membrane protein assembly machine. *Science* 317(5840): 961-964.

9. Bos MP, Tefsen B, Geurtsen J, Tommassen J (2004) Identification of an outer membrane protein required for the transport of lipopolysaccharide to the bacterial cell surface. *Proc Natl Acad Sci USA* 101(25): 9417-9422.

10. Wu T, et al. (2006) Identification of a protein complex that assembles lipopolysaccharide in the outer membrane of *Escherichia coli*. *Proc Natl Acad Sci USA* 103(31): 11754-11759.31.

11. Sperandeo P, et al. (2007) Characterization of *lptA* and *lptB*, two essential genes implicated in lipopolysaccharide transport to the outer membrane of *Escherichia coli*. *J Bacteriol* 189(1): 244-253.

12. Sperandeo P, et al. (2008) Functional analysis of the protein machinery required for transport of lipopolysaccharide to the outer membrane of *Escherichia coli*. *J Bacteriol* 190(13): 4460-4469.

13. Ruiz N, Gronenberg LS, Kahne D, Silhavy TJ (2008) Identification of two inner-membrane proteins required for the transport of lipopolysaccharide to the outer membrane of *Escherichia coli*. *Proc Natl Acad Sci USA* 105(14): 5537-5542.

14. Narita S, Tokuda H (2009) Biochemical characterization of an ABC transporter LptBFGC complex required for the outer membrane sorting of lipopolysaccharides. *FEBS Lett* 583(13): 2160-2164.

15. Chimalakonda G, et al. (2011) Lipoprotein LptE is required for the assembly of LptD by the beta-barrel assembly machine in the outer membrane of *Escherichia coli*. *Proc Natl Acad Sci USA* 108(6): 2492-2497.

16. Freinkman E, Chng SS, Kahne D (2011) The complex that inserts lipopolysaccharide into the bacterial outer membrane forms a two-protein plug-and-barrel. *Proc Natl Acad Sci USA* 108(6): 2486-2491.

17. Chng SS, et al. (2012) Disulfide rearrangement triggered by translocon assembly controls lipopolysaccharide export. *Science* 337(6102): 1665-1668.

18. Kadokura H, Tian H, Zander T, Bardwell JC, Beckwith J (2004) Snapshots of DsbA in action: detection of proteins in the process of oxidative folding. *Science* 303(5657): 534-537.

19. Ruiz N, Chng SS, Hiniker A, Kahne D, Silhavy TJ (2010) Nonconsecutive disulfide bond formation in an essential integral outer membrane protein. *Proc Natl Acad Sci USA* 107(27): 12245-12250.

20. Denoncin K, Vertommen D, Paek E, Collet JF (2010) The protein-disulfide isomerase DsbC cooperates with SurA and DsbA in the assembly of the essential β-barrel protein LptD. *J Biol Chem* 285(38): 29425-29433.

21. Rowley G, Spector M, Kormanec J, Roberts M (2006) Pushing the envelope: extracytoplasmic stress responses in bacterial pathogens. *Nat Rev Microbiol* 4(5): 383-394.

22. Walsh NP, Alba BM, Bose B, Gross CA, Sauer RT (2003) OMP peptide signals initiate the envelope-stress response by activating DegS protease via relief of inhibition mediated by its PDZ domain. *Cell* 113(1): 61-71.

23. Lima S, Guo MS, Chaba R, Gross CA, Sauer RT (2013) Dual molecular signals mediate the bacterial response to outer-membrane stress. *Science* 340(6134): 837-841.

24. Bury-Moné S, et al. (2009) Global analysis of extracytoplasmic stress signaling in *Escherichia coli*. *PLoS Genet* 5(9): e1000651.

25. Spiess C, Beil A, Ehrmann M (1999) A temperature-dependent switch from chaperone to protease in a widely conserved heat shock protein. Cell 97(3): 339-347.

26. Misra R, CastilloKeller M, Deng M (2000) Overexpression of protease-deficient DegP(S210A) rescues the lethal phenotype of *Escherichia coli* OmpF assembly mutants in a *degP* background. *J Bacteriol* 182(17): 4882-4888.

27. Krojer T, et al. (2008) Structural basis for the regulated protease and chaperone function of DegP. *Nature* 453(7197): 885-890.

28. Girgis HS, Hottes AK, Tavazoie S (2009) Genetic architecture of intrinsic antibiotic susceptibility. *PLoS One* 4(5): e5629.

29. Liu A, et al. (2010) Antibiotic sensitivity profiles determined with an *Escherichia coli* gene knockout collection: generating an antibiotic bar code. *Antimicrob Agents Chemother* 54(4): 1393-1403.

30. Nichols RJ, et al. (2011) Phenotypic landscape of a bacterial cell. *Cell* 144(1): 143-156.

31. Oh E, et al. (2011) Selective ribosome profiling reveals the cotranslational chaperone action of trigger factor *in vivo*. *Cell* 147(6): 1295-1308.

32. Allan RK, Ratajczak T (2011) Versatile TPR domains accommodate different modes of target protein recognition and function. *Cell Stress Chaperones* 16(4): 353-367.

33. Ehses S, et al. (2009) Regulation of OPA1 processing and mitochondrial fusion by m-AAA protease isoenzymes and OMA1. *J Cell Biol* 187(7): 1023-1036.

34. Fujimura-Kamada K, Nouvet FJ, Michaelis S (1997) A novel membrane-associated metalloprotease, Ste24p, is required for the first step of NH_2-terminal processing of the yeast a-factor precursor. *J Cell Biol* 136(2): 271-285.

35. Sakoh M, Ito K, Akiyama Y (2005) Proteolytic activity of HtpX, a membrane-bound and stress-controlled protease from *Escherichia coli*. *J Biol Chem* 280(39): 33305-33310.

36. Akiyama Y (2009) Quality control of cytoplasmic membrane proteins in *Escherichia coli*. *J Biochem* 146(4): 449-454.

37. Lütticke C, et al. (2012) *E. coli* LoiP (YggG), a metalloprotease hydrolyzing Phe-Phe bonds. *Mol Biosyst* 8(6): 1775-1782.

38. Kitagawa M, et al. (2005) Complete set of ORF clones of *Escherichia coli* ASKA library (a complete set of *E. coli* K-12 ORF archive): unique resources for biological research. *DNA Res* 12(5): 291-299.

39. Chng SS, Ruiz N, Chimalakonda G, Silhavy TJ, Kahne D (2010) Characterization of the two-protein complex in *Escherichia coli* responsible for lipopolysaccharide assembly at the outer membrane. *Proc Natl Acad Sci USA* 107(12): 5363-5368.

40. Hirokawa T, Boon-Chieng S, Mitaku S (1998) SOSUI: classification and secondary structure prediction system for membrane proteins. *Bioinformatics* 14(4): 378-379.

41. Young TS, Ahmad I, Yin JA, Schultz PG (2010) An enhanced system for unnatural amino acid mutagenesis in *E. coli*. *J Mol Biol* 395(2): 361-374.

42. Hagan CL, Kim S, Kahne D (2010) Reconstitution of outer membrane protein assembly from purified components. *Science* 328(5980): 890-892.

43. Sklar JG, Wu T, Kahne D, Silhavy TJ (2007) Defining the roles of the periplasmic chaperones SurA, Skp, and DegP in *Escherichia coli*. *Genes Dev* 21(19): 2473-2484.

44. Tellez R Jr, Misra R (2012) Substitutions in the BamA β-barrel domain overcome the conditional lethal phenotype of a Δ*bamB* Δ*bamE* strain of *Escherichia coli*. *J Bacteriol* 194(2): 317-324.

45. Rigel NW, Schwalm J, Ricci DP, Silhavy TJ (2012) BamE modulates the *Escherichia coli* beta-barrel assembly machine component BamA. *J Bacteriol* 194(5): 1002-1008.

46. Rigel NW, Ricci DP, Silhavy TJ (2013) Conformation-specific labeling of BamA and suppressor analysis suggest a cyclic mechanism for β-barrel assembly in *Escherichia coli*. *Proc Natl Acad Sci USA* 110(13): 5151-5156.

47. Kadokura H, Beckwith J (2009) Detecting folding intermediates of a protein as it passes through the bacterial translocation channel. *Cell* 138(6): 1164-1173.

48. Ruiz N, Kahne D, Silhavy TJ (2009) Transport of lipopolysaccharide across the cell envelope: the long road of discovery. *Nat Rev Microbiol* 7(9): 677-683.

49. Weski J, Ehrmann M (2012) Genetic analysis of 15 protein folding factors and proteases of the *Escherichia coli* cell envelope. *J Bacteriol* 194(12): 3225-3233.

50. Kihara A, Akiyama Y, Ito K (1995) FtsH is required for proteolytic elimination of uncomplexed forms of SecY, an essential protein translocase subunit. *Proc Natl Acad Sci USA* 92(10): 4532-4536.

51. Casadaban MJ (1976) Transposition and fusion of the *lac* genes to selected promoters in *Escherichia coli* using bacteriophage lambda and Mu. *J Mol Biol* 104(3): 541-555.

52. Baba T, et al. (2006) Construction of *Escherichia coli* K-12 in-frame, single-gene knockout mutants: the Keio collection. *Mol Syst Biol* 2: 2006.0008.

53. Miller JH (1972) Experiments in Molecular Genetics. Cold Spring Harbor Laboratory Press, Cold Spring Harbor, NY.

Figure legends

Fig. 1. Protease activity is required for BepA function. (*A*) Protease activity of BepA. α-casein (400 μg/mL) was incubated without (-) or with His_{10}-tagged wild-type BepA (WT) or its E137Q derivative (E137Q) (200 μg/mL) at 37°C for 0 or 24 h. Proteins were separated by SDS-PAGE and visualized by staining with Coomassie brilliant blue R-250. Proteolytic product of α-casein is indicated by an open arrowhead. Migration positions of molecular weight markers are shown on the left. (*B*) Effects of metal chelators on the BepA protease activity. Protease activity of C-terminally His_{10}-tagged wild-type BepA was analyzed as in *A* except that the reaction mixture contained 50 μM $ZnCl_2$ (Zn), 250 μM 1,10-Phenanthroline (PT), or 250 μM EDTA. (*C*) Erythromycin sensitivity of cells expressing BepA or its derivative. The minimum inhibitory concentration (MIC) of erythromycin for the Δ*bepA* or wild-type strain transformed with pUC18 vector, pUC-bepA, pUC-bepA(H136R), or pUC-bepA(E137Q) encoding wild-type, H136R mutant, or E137Q mutant BepA, respectively, at 30°C are shown. (*D*) Cellular levels of BepA. BepA levels in the Δ*bepA* cells used in (*C*) were determined by immunoblotting with anti-BepA antiserum. Maltose-binding protein (MBP) was also detected by immunoblotting with anti-MBP antibodies and was used as a loading control.

Fig. 2. Overexpression of LptE suppresses the drug sensitivity of the Δ*bepA* strain. (*A*) Erythromycin sensitivity of the Δ*bepA* strain transformed with an ASKA clone carrying *lptE*. pCA24NΔNot was used as a vector control. For comparison, the MIC of the Δ*bepA* strain transformed with pTH-bepA-his$_{10}$ encoding wild-type BepA$_{His10}$ is shown. (*B*) LptE was overexpressed from pMAN-lptE carrying *lptE* under the control of the *araBAD* promoter. Expression of LptE was confirmed by SDS-PAGE of total cellular proteins followed by anti-LptE immunoblotting.

Fig. 3. Defective oxidative folding of LptD in the absence of BepA. (*A*) Immunoblotting of LptD was carried out after reducing (+ME) or nonreducing (-ME) SDS-PAGE of total cellular proteins. Wild-type (+) or Δ*bepA* (-) cells were grown overnight at 30°C. Anti-LptE immunoblotting was also carried out after reducing SDS-PAGE. The positions of reduced LptD (LptD^{RED}), properly oxidized LptD (LptD^{NC}), rapidly migrating LptD (LptD^{C}), LptE, and molecular weight markers are indicated. (*B*) Schematic representation of disulfide bonds in LptD^{NC} and LptD^{C}. Asterisk indicates a nonspecific band.

Fig. 4. BepA facilitates disulfide isomerization in LptD. (*A*) Wild-type and Δ*bepA* cells were labeled with [^{35}S]-methionine for 1 min and chased for the indicated durations at 30°C. Acid-precipitated proteins were subjected to immunoprecipitation with anti-LptD antiserum and were analyzed by nonreducing (-ME) or reducing (+ME) SDS-PAGE followed by phosphorimaging. Migration positions of molecular weight markers are shown on the left. (*B*) Oxidative folding of LptD was monitored as in (*A*) using Δ*bepA* cells transformed with empty vector or either of the plasmids encoding C-terminally His$_{10}$-tagged wild-type BepA or its H136R or E137Q derivative. LptD^{NC} (%) in the right panels was calculated by dividing the band intensity of LptD^{NC} by the sum of those of LptD^{C} and LptD^{NC}.

Fig. 5. BepA destabilizes LptD in LptE-limiting conditions. (*A*) LptE-depleted cells carrying *bepA* (*bepA^{+}*) or its disruptant were pulse-labeled and analyzed as described in the legend to Fig. 4*A*. (*B* and *C*) The stability of LptD was assessed as in (*A*) using the Δ*bepA* (*B*) or wild-type (*C*) cells transformed with empty vector or either of the plasmids encoding C-terminally His$_{10}$-tagged wild-type BepA or its H136R or E137Q derivative.

Fig. 6. *bamB/bepA* and *bamE/bepA* double disruptants show elevated drug sensitivity. (*A*) MICs of erythromycin (ERM), rifampicin (RIF), vancomycin (VCN), and novobiocin (NOV) at 30°C

for strains lacking *bepA*, *bamB*, *bamC*, and *bamE* individually or in combinations as indicated.

(*B*) Overnight cultures of strains lacking *bepA*, *bamB*, *bamC*, and *bamE* individually or in combinations as indicated were serially diluted with saline, spotted onto L agar with or without 0.5% SDS, and incubated at 30°C for 24 h. (*C*) *bamB*/*bepA* and *bamE*/*bepA* double-knockout strains were transformed with a plasmid encoding wild-type BepA or its H136R or E137Q derivative and were grown on L agar containing 0.5% SDS for 24 h at 30°C or 37°C.

Fig. 7. BepA interacts with the BAM complex. (*A*-*G*) BS^3-mediated cross-linking. (*A* and *B*) Wild-type cells transformed with the pUC18 vector (-) or its derivative encoding the C-terminally His$_{10}$-tagged wild-type BepA (WT) or its H136R or E137Q derivative were subjected to cross-linking with BS^3 as described in the *Materials and Methods* section. Membrane (M) and periplasmic (P) fractions were analyzed to SDS-PAGE followed by immunoblotting with anti-BepA (*A*) or anti-BamA (*B*) antisera. The cross-linked product of BepA and BamA is indicated (× BamA; also indicated by asterisks). (*C*–*G*) The Δ*bepA* strain (WT) or the Δ*bepA* strain also having deletions of *bamB* (Δ*B*), *bamC* (Δ*C*), or *bamE* (Δ*E*) were transformed with empty vector (-) or a plasmid encoding tag-free BepA(E137Q) and were subjected to BS^3 cross-linking. Membrane fractions were analyzed by WIDE RANGE PAGE (Nacalai Tesque, Kyoto, Japan) (7.5% acrylamide), except for (*D*), in which normal SDS-PAGE was employed, followed by immunoblotting with anti-BepA (*C*), anti-BamA (*D*), anti-BamB (*E*), anti-BamC (*F*), or anti-BamD (*G*) antisera. (*H*) Photo-crosslinking of BepA and BamA. The Δ*bepA* cells transformed with pEVOL-pBpF (aminoacyl-tRNA synthetase/suppressor tRNA) and the plasmid encoding a BepA derivative with an amber codon at position 428 were grown with or without pBPA and were UV-irradiated for 10 min. Acid precipitated proteins were analyzed by SDS-PAGE and immunoblotting with anti-BepA and anti-BamA antisera. The cross-linked product between BepA(Q428pBPA) and BamA is indicated. (*I*) Pull-down

assay. Wild-type strain (WT) transformed with empty vector or the Δ*bamB* strain transformed with a plasmid encoding C-terminally His$_6$-tagged BamB (BamB$_{His6}$) were co-transformed with a plasmid encoding BepA(E137Q). Membrane proteins were solubilized and subjected to a pull-down assay using His$_6$ tag of BamB. Solubilized membrane (input) and affinity-purified proteins (eluate, a fivefold equivalent for Bam component immunoblotting and a 50-fold equivalent for BepA and OmpA immunoblotting) were analyzed by SDS-PAGE and immunoblotting.

Fig. 8. BepA-dependent degradation of BamA in the Δ*surA* strain. Total cellular protein was prepared from wild-type or mutant cells lacking *bepA* and/or *surA* (lanes 1–4) or Δ*surA*/Δ*bepA* cells harboring empty vector or either of the plasmids encoding C-terminally His$_{10}$-tagged wild-type BepA or its H136R or E137Q derivative (lanes 5–8) and was subjected to SDS-PAGE followed by immunoblotting with anti-BamA or anti-BepA antisera. Putative BepA degradation products of BamA are indicated by asterisks.

Fig. 9. A model for BepA function in the assembly/degradation of the OM LPS translocon. (upper panel) BepA promotes disulfide rearrangement of LptD^C that is triggered by association of LptD^C with LptE. BepA may directly assist LptD-LptE interaction or act indirectly to facilitate formation of the productive LptD-LptE complex. Square brackets represent disulfide bonds (lower panel). In the absence of LptE, BepA acts to proteolytically eliminate accumulated LptD^C.

Supporting Information

SI Materials and Methods

Bacterial strains

SN1145 was constructed by removing the kanamycin-resistance cassette from GC187 by using pCP20. Gene disruption of AD16, MC4100, and SN1145 was conducted by transferring the kanamycin-resistance cassette from a corresponding strain of the Keio collection by P1-mediated transduction (1). Multiple-gene disruptants were constructed by successive transduction combined with removal of the kanamycin-resistance cassette by using pCP20 as described previously (2). SN147, SN150, and SN909 were constructed by transducing the $\Delta bamB$::tet allele from SM4106 to AD16, SN56, and SN896, respectively, by P1 transduction. All gene disruptions were verified by PCR with appropriate primers.

Plasmids

For construction of pCA24NΔNot, which was used as an empty vector control for ASKA plasmids, a NotI fragment was deleted from pCA24N (3) by digestion with NotI followed by self-ligation. pUC-bepA-his$_6$ was constructed as follows. A DNA fragment encoding BepA$_{His6}$ was amplified by PCR from the genomic DNA of $E.\ coli$ BW25113 (4) using a pair of primers, yfgC-1 and yfgC-2 (Supplemental Table S3). The amplified DNA fragment was digested with EcoRI and KpnI and then cloned into the same sites of pUC18. pTTQ-bepA-his$_6$ was constructed essentially as described for pUC-bepA-his$_6$ except that the DNA fragment was amplified with yfgC-3 instead of yfgC-1 and cloned into pTTQ18. pUC-bepA-his$_{10}$ was constructed by self-ligation of a DNA fragment that was PCR-amplified from pUC-bepA-his$_6$ using a pair of primes, yfgC-his10-1 and yfgC-his10-2, after treatment with T4 polynucleotide

kinase (TaKaRa Bio, Otsu, Japan). pTH-bepA-his$_{10}$ was constructed by subcloning the

EcoRI-SalI fragment derived from pUC-bepA-his$_{10}$ into the same sites of pTH18cr. For

construction of pCDF-bepA-his$_{10}$, a DNA fragment was PCR-amplified from pUC-bepA-his$_{10}$

using a pair of primers, yfgC-4 and M4C, digested with NcoI and SalI, and cloned into the same

sites of pCDFDuet-1. For construction of pUC-bepA, a DNA fragment was PCR-amplified

from pTH-bepA-his$_{10}$ using a pair of primers, yfgC-1 and yfgC-Pst-2, and cloned into the

EcoRI-SmaI site of pUC18 after digestion with EcoRI. Plasmids encoding the H136R mutant

form of BepA were constructed by site-directed mutagenesis using a pair of complementary

primers, yfgC_H136R and yfgC_H136R-r. Plasmids encoding the E137Q mutant form of BepA

were constructed in the same way using primers yfgC_E137X and yfgC_E137X-r.

pUC-bepA(Q428Amber) was also constructed in the same way using primers TPR4-2 and

TPR4-2-r. pMAN-lptE was constructed as follows. The lptE coding region was PCR-amplified

from the genomic DNA of BW25113 using a pair of primers, lptE-1 and lptE-2. The amplified

DNA fragment was digested with EcoRI and HindIII, and then cloned into the same sites of

pMAN885EH. To construct pMAN-lptD-his$_6$, a DNA fragment encoding LptD$_{His6}$ was

amplified by PCR from the genomic DNA of BW25113 using a pair of primers, lptD-1 and

lptD-2, digested with XbaI, and cloned into the SmaI-XbaI site of pMAN885EH.

pMAN-lptD-his$_6$ derivatives encoding LptD$_{His6}$ with Cys to Ser substitutions were constructed

by site-directed mutagenesis. To construct pMAN-bamB-his$_6$, a DNA fragment encoding

BamB$_{His6}$ was amplified by PCR from the genomic DNA of DH5α using a pair of primers,

yfgL-1 and yfgL-2, digested with EcoRI and HindIII, and cloned into the same sites of

pMAN885EH.

Purification of BepA and *in vitro* proteolytic activity assay

KRX cells were transformed with pCDF-bepA-his$_{10}$ or pCDF-bepA(E137Q)-his$_{10}$ encoding

His$_{10}$-tagged wild-type BepA or BepA(E137Q) and grown in L medium supplemented with 0.1% rhamnose at 37°C. When the culture OD (at 600 nm) reached 1.0, cells were harvested by centrifugation at 5,000 × g for 10 min, and then resuspended in 20 mM Tris–HCl (pH 7.5) containing 1 μg/mL DNase I. Cells were disrupted by a single passage through a French Press cell at 10,000 psi. After removal of unbroken cells by centrifugation at 10,000 × g for 5 min, membranes were removed by centrifugation at 100,000 × g for 1 h. The supernatant was applied to TALON metal affinity resin (Clontech), and the column was successively washed with buffer A (20 mM Tris–HCl (pH 7.5), 50 mM NaCl) supplemented with 0, 5, or 20 mM imidazole, and finally eluted with buffer A containing 50 mM imidazole.

For protease activity assay, a purified preparation of BepA$_{His10}$ or BepA(E137Q)$_{His10}$ (200 μg/mL) was mixed with α-casein (400 μg/mL; Sigma) and incubated at 37°C in buffer containing 20 mM Tris-HCl (pH 7.5), 0.05% n-dodecyl-β-D-maltopyranoside (DDM), and 10 μM ZnCl$_2$. Where specified, 1,10-phenanthroline or EDTA instead of ZnCl$_2$ was added at 250 μM. Samples were mixed with a quarter volume of 5× SDS sample buffer, boiled for 5 min, and subjected to SDS-PAGE. Proteins were visualized by staining with Coomassie brilliant blue R-250 (CBB).

Pull-down assay

Cells of AD16 transformed with pMAN885EH and pUC-bepA(E137Q), and SN147 transformed with pMAN-bamB-his$_6$ and pUC-bepA(E137Q), were grown in L medium supplemented with 0.01% arabinose and 0.1 mM IPTG at 30°C. When the culture OD reached 1.0, cells were harvested by centrifugation at 5,000 × g for 10 min, and resuspended in 20 mM Tris–HCl (pH 7.5) containing 1 μg/mL DNase I. Cells were disrupted by a single passage through a French Press cell at 10,000 psi. After removal of unbroken cells by centrifugation at 10,000 × g for 5 min, the membrane fraction was recovered by centrifugation at 100,000 × g for

1 h. The membranes were resuspended in 20 mM Tris-HCl (pH 7.5) containing 300 mM NaCl and 2% (w/v) DDM, and incubated at 4°C for 30 min for solubilization. After removal of insoluble materials by centrifugation at 100,000 × g for 30 min, the supernatant was diluted 10 fold with 20 mM Tris-HCl (pH 7.5) containing 300 mM NaCl and applied to Dynabeads His-tag Isolation & Pulldown (Invitrogen). The beads were successively washed with buffer B (20 mM Tris–HCl (pH 7.5), 300 mM NaCl, 0.05% DDM), supplemented with 0, 5, 20, or 50 mM imidazole, and eluted with buffer B containing 250 mM imidazole.

Mass spectrometry

The membrane fraction of bis(sulfosuccinimidyl) suberate (BS^3)-treated spheroplasts of MC4100 transformed with pTTQ-bepA(E137Q)-his_6 was prepared as described above and solubilized in 50 mM Tris-HCl (pH 7.5) containing 0.5% SDS at 37°C for 5 min. After 10-fold dilution with 20 mM Tris-HCl (pH 7.5) containing 2% Triton X-100, insoluble materials were removed by ultracentrifugation at 100,000 × g for 30 min, and the supernatant was mixed with Ni-NTA agarose resin (Qiagen) for 1 h at 4°C. Resin was washed with 20 mM Tris-HCl (pH 7.5) containing 300 mM NaCl, 0.2% (w/v) Triton X-100, and either 0, 5, or 20 mM imidazole, and bound BepA$_{His6}$ was eluted with 20 mM Tris-HCl (pH 7.5) containing 300 mM NaCl and 250 mM imidazole. The cross-linked product containing BepA was visualized by staining with CBB after SDS-PAGE. An excised CBB-stained gel band was destained with 50% (v/v) acetonitrile in 10 mM Tris-HCl (pH 8.0) and then dried *in vacuo*. The band was incubated with 0.01 μg trypsin, TPCK-treated (Worthington Biochemical Corporation, Lakewood, NJ) in 10 mM Tris-HCl (pH 8.0) at 37°C for 12 h. An aliquot of the digest was analyzed by nano LC-MS/MS using an LCQ Deca XP instrument (Thermo Fisher Scientific). The peptides were separated using a nano ESI spray column (100 μm i.d. × 375 μm o.d.) packed with a reversed-phase material (Inertsil ODS-3, 3 μm, GL Science, Tokyo, Japan) at a flow rate of 200

nL/min. The mass spectrometer was operated in the positive-ion mode, and the spectra were

acquired in a data-dependent MS/MS mode. The MS/MS spectra were searched against the

NCBInr 20111107 database (15,916,306 sequences; 5,467,648,827 residues) using an in-house

MASCOT server (version: 2.2.1, Matrix Science, London, UK).

Alkylation of LptD$_{His6}$

Cells of AD16 transformed with pMAN885EH derivatives encoding wild-type LptD$_{His6}$,

LptD(SSCC)$_{His6}$, or LptD(CCSS)$_{His6}$ were grown overnight in L medium at 30°C. They were

harvested, resuspended in 100 mM Tris-HCl (pH 8.0), and incubated in the absence or presence

of 100 mM DTT at room temperature for 30 min. Total cellular proteins were precipitated by

trichloroacetic acid treatment and solubilized with 100 mM Tris-HCl (pH 8.0) containing 1%

SDS by vortexing at room temperature for 30 min. Samples were incubated in the absence or

presence of 10 mM EZ-Link Maleinide-PEG$_2$-Biotin (Thermo Fisher Scientific) at 37°C for 30

min. Proteins were separated by SDS-PAGE, and LptD$_{His6}$ was detected by immunoblotting

with anti-His antibodies.

Cell fractionation

Subcellular localization of LptD was determined as follows. Cells of AD16 and SN56 (Δ*bepA*)

were grown overnight in L medium at 30°C. They were harvested, resuspended in 20 mM

Tris-HCl (pH 7.5) containing 1 mM Pefabloc (Merck) and 100 μg/mL lysozyme, and subjected

to freezing and thawing. Then, 10 μg/mL DNase I was added to the samples, and cells were

disrupted by sonication. After removal of unbroken cells, membranes were recovered by

centrifugation at 100,000 × g for 1 h at 4°C and suspended in 20 mM Tris-HCl (pH 7.5)

containing 1 mM EDTA and 1 mM Pefabloc. The supernatant was saved as the soluble fraction.

Total membranes thus obtained were layered on a 30–55% (w/w) stepwise sucrose gradient and

centrifuged at 60,000 × g for 12 h at 4°C. The sucrose gradient was fractionated into portions and analyzed by SDS-PAGE and immunoblotting.

Growth of LptE-deficient strains

Cells of GC187 and their derivatives were grown overnight in M9 medium supplemented with 19 amino acids other than methionine, 2 μg/mL thiamine, 0.2% arabinose, and 0.2% glucose or maltose. Cells from 1-mL aliquots cultures were pelleted, washed three times with equal volumes of the same medium without arabinose, and inoculated into the same medium without arabinose to an initial OD_{600} of ~0.001. Cells were subsequently grown at 30°C to an early log phase.

Other techniques

The minimum inhibitory concentrations (MICs) of antibiotics were determined by the agar dilution method using L agar. SDS-PAGE was carried out as described (5), unless otherwise specified. WIDE RANGE Gel Preparation buffer (Nacalai Tesque, Kyoto, Japan) was used in some experiments to improve separation of proteins. To raise anti-BepA antibodies, $BepA_{His6}$ was purified from SN150 carrying pTTQ-bepA-his$_6$ by metal affinity chromatography using TALON resin (Clontech) and used to immunize rabbits. A Penta-His HRP Conjugate Kit (Qiagen) or anti-His-tag polyclonal antibodies (MBL, Nagoya, Japan) were used to probe polyhistidine-tagged proteins. Anti-BamA, -BamB, -BamD, -LptD, and -LptE antisera were provided by Dr. Shin-ichi Matsuyama (Rikkyo University). Anti-BamC and -LamB antisera were provided by Dr. Thomas J. Silhavy (Princeton University). Anti-OmpA antiserum was provided by Dr. Hajime Tokuda (University of Morioka). Anti-MBP antiserum was purchased from MBL. Immunoblotting was carried out essentially as described previously (6), and proteins were visualized using enhanced chemiluminescence substrate (ECL or ECL Prime; GE

Healthcare), followed by detection with a lumino-image analyzer (LAS-3000mini; Fujifilm).

1. Miller JH (1972) Experiments in Molecular Genetics. Cold Spring Harbor Laboratory Press, Cold Spring Harbor, NY.

2. Cherepanov PP, Wackernagel W (1995) Gene disruption in *Escherichia coli*: Tc^R and Km^R cassettes with the option of Flp-catalyzed excision of the antibiotic-resistance determinant. *Gene* 158(1): 9-14.

3. Kitagawa M, et al. (2005) Complete set of ORF clones of *Escherichia coli* ASKA library (a complete set of *E. coli* K-12 ORF archive): unique resources for biological research. *DNA Res* 12(5): 291-299.

4. Baba T, et al. (2006) Construction of *Escherichia coli* K-12 in-frame, single-gene knockout mutants: the Keio collection. *Mol Syst Biol* 2: 2006.0008.

5. Laemmli UK (1970) Cleavage of structural proteins during the assembly of the head of bacteriophage T4. *Nature* 227(5259): 680-685.

6. Shimoike T, et al. (1995) Product of a new gene, *syd*, functionally interacts with SecY when overproduced in *Escherichia coli*. *J Biol Chem* 270(10): 5519-5526.

Legends to SI Figures

Fig. S1. Membrane protein profiles of the wild-type and Δ*bcpA* strains. Crude membranes prepared from overnight cultures of wild-type (+) or Δ*bcpA* cells (-) were solubilized in a SDS-PAGE sample buffer with (+) or without (-) heating at 99°C for 5 min and were analyzed by the WIDE RANGE PAGE (10% acrylamide) followed by CBB staining.

Fig. S2. Connectivity of disulfide bonds and subcellular localization of LptD^C. (*A*) Cells of wild-type or Δ*bepA* strains were transformed with plasmids encoding C-terminally His$_6$-tagged LptD (LptD$_{His6}$) with Cys to Ser substitutions. Total cellular proteins were acid precipitated and analyzed by nonreducing (-ME) or reducing (+ME) SDS-PAGE and immunoblotting with anti-His-tag antibodies. Asterisks indicate LptD$_{His6}$ with a disulfide bond of C$_{31}$-C$_{724}$ (*), C$_{173}$-C$_{724}$ or C$_{173}$-C$_{725}$ (**), or C$_{724}$-C$_{725}$ (***), while bullets indicate a degradation product of LptD$_{His6}$. (*B*) Sulfhydryl modification. Wild-type cells transformed with a plasmid encoding wild-type LptD$_{His6}$ (denoted as CCCC) or LptD$_{His6}$ with C$_{31}$S/C$_{173}$S substitutions (SSCC) or C$_{724}$S/C$_{725}$S substitutions (CCSS) were incubated in the presence or absence of DTT. Acid-denatured cellular proteins were labeled with maleimide-PEG$_2$-biotin (MB), and analyzed by reducing SDS-PAGE followed by immunoblotting with anti-His antibodies. (*C*) Subcellular localization of LptD^C. Wild-type (+) or Δ*bepA* (-) cells were fractionated into membrane (M) and soluble (S) fractions. Anti-LptD, anti-MBP, or anti-FtsH immunoblotting was carried out after nonreducing SDS-PAGE. FtsH (7) and MBP were detected as markers for membrane and soluble fractions, respectively. (*D*) Membranes of Δ*bepA* cells were fractionated into the IM and OM by sucrose gradient centrifugation. Proteins of each fraction were analyzed by nonreducing SDS-PAGE and immunoblotting with anti-LptD antiserum. FtsH was used as a marker for the IM.

Fig. S3. Dominant-negative effect of the BepA protease active-site mutants on disulfide isomerization of LptD. Oxidative folding of LptD was monitored using wild-type cells transformed with either of the plasmids encoding C-terminally His$_{10}$-tagged wild-type BepA or its H136R or E137Q derivative.

Fig. S4. Overexpression of LptE facilitates disulfide isomerization in LptD. (*A*) Immunoblotting analysis. Δ*bepA* cells were transformed with an empty vector or pMAN-lptE carrying *lptE* under the control of the *araBAD* promoter and grown in the absence (-) or presence (+) of 0.2% arabinose. Immunoblotting of LptD was carried out after nonreducing SDS-PAGE of total cellular proteins. (*B*) Pulse-chase analysis. Oxidative folding of LptD was monitored as in Fig. 4 using Δ*bepA* cells transformed with an empty vector or pMAN-lptE grown in M9 medium supplemented with 0.2% glucose (- ara) or 0.2% maltose plus 0.2% arabinose (+ ara).

Fig. S5. Disulfide isomerization of LptD in the cells lacking periplasmic oxidoreductases. (*A*) Effects of the *dsbC* and *dsbD* disruption. Oxidative folding of LptD was monitored as in Fig. 4 using *dsbC* and/or *dsbG* knockout cells carrying wild-type *bepA* or its disruptant. (*B*) Effects of the *dsbA* disruption. *dsbA* knockout cells additionally lacking *dsbC*, *dsbG*, and/or *bepA* as indicated were analyzed as in (*A*) with nonreducing (-ME) or reducing (+ME) SDS-PAGE.

Fig. S6. Subcellular localization of BepA. Wild-type (+) or Δ*bepA* (-) cells were disrupted by sonication and fractionated into membrane (M) and soluble (S) fractions by ultracentrifugation. Each protein was detected by SDS-PAGE and immunoblotting with antiserum against respective proteins.

Fig. S7. Purification of the BS^3-mediated cross-linked product. Spheroplasts of wild-type cells transformed with a plasmid encoding C-terminally His$_6$-tagged BepA with E137Q substitution

were treated with BS^3. BepA(E137Q)$_{His6}$ and its cross-linked products were affinity purified as described in the *Materials and Methods* section and visualized by staining with CBB after SDS-PAGE. The cross-linked product (× BamA) that was subsequently identified as the BamA-BepA adduct by mass spectrometry is indicated.

Fig. S8. Effect of the *surA* disruption or BepA overproduction on the OM protein profiles. (*A and B*) Effect on LamB and OmpA. Total cellular protein was prepared from Δ*surA*/Δ*bepA* cells harboring empty vector or either of the plasmids encoding C-terminally His$_{10}$-tagged wild-type BepA or its H136R or E137Q derivative and was subjected to SDS-PAGE followed by immunoblotting with anti-LamB (*A*) or anti-OmpA (*B*) antisera. (*C*) Effect on BamA. Overexpression of BepA does not cause the degradation of BamA in the *surA*$^+$ cells. Total cellular proteins were prepared from wild-type (lanes 1, 3-6) or the Δ*surA* cells (lane 2) without plasmid (lanes 1 and 2) or with either empty vector or a plasmid encoding C-terminally His$_{10}$-tagged wild-type BepA or its H136R or E137Q derivative (lanes 3–6) and was subjected to SDS-PAGE followed by immunoblotting with anti-BamA or anti-BepA antisera. Putative BepA degradation products of BamA are indicated by asterisks.
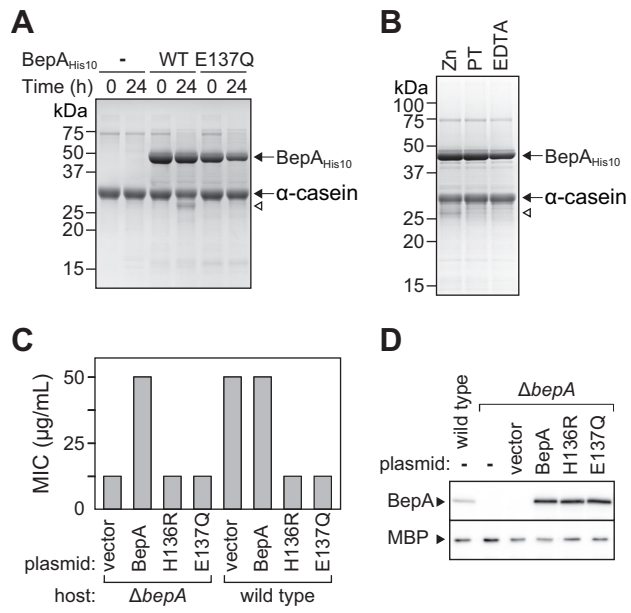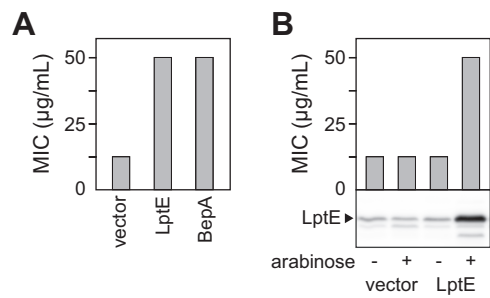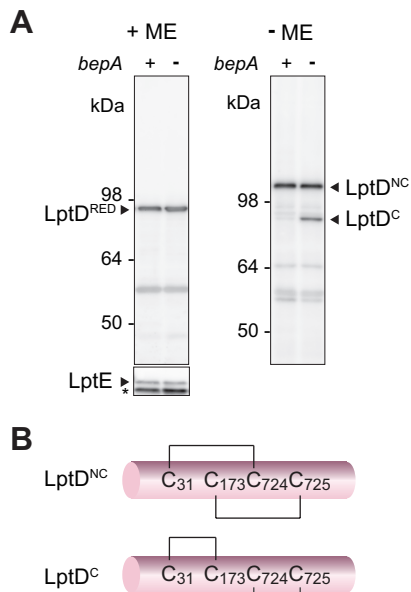
A

BepA$_{His10}$ - WT E137Q
Time (h) 0 24 0 24 0 24
kDa
75
50 ← BepA$_{His10}$
37
← α-casein
25
20 ◁
15

B

Zn PT EDTA
kDa
100
75
50 ← BepA$_{His10}$
37
← α-casein
25 ◁
20
15

C

MIC (μg/mL)
50
25
0
plasmid: vector BepA H136R E137Q vector BepA H136R E137Q
host: ΔbepA wild type

D

wild type ΔbepA
plasmid: - - vector BepA H136R E137Q
BepA ▶
MBP ▶

Fig. 1

A

MIC (μg/mL)
50
25
0
vector LptE BepA

B

MIC (μg/mL)
50
25
0
LptE ▶
arabinose - + - +
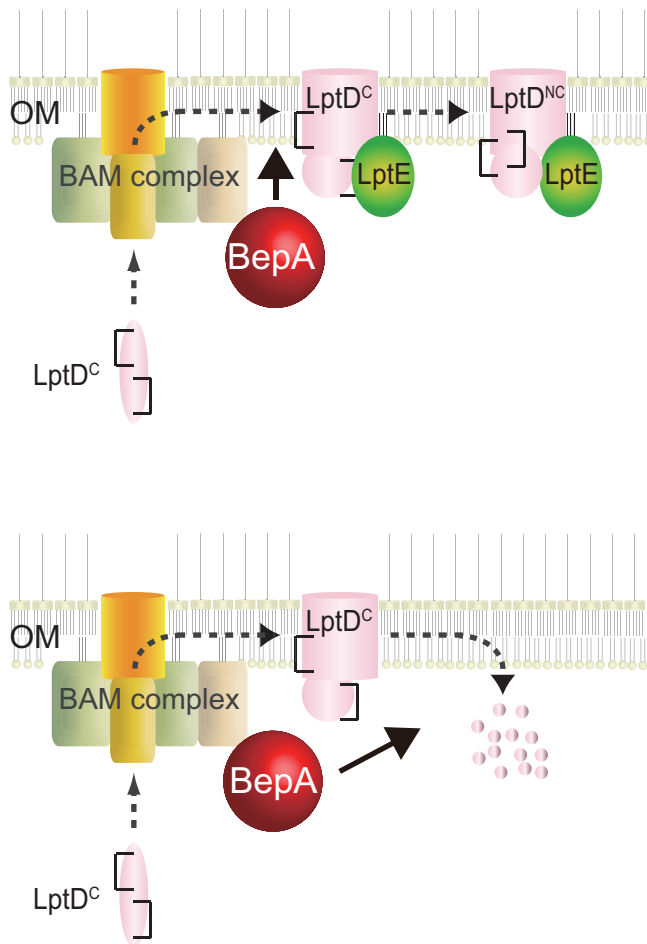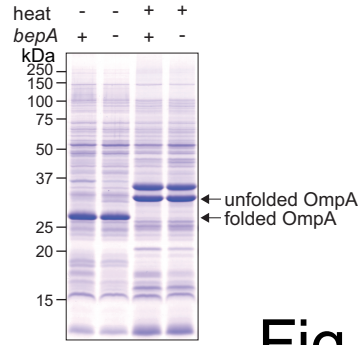vector LptE

Fig. 2
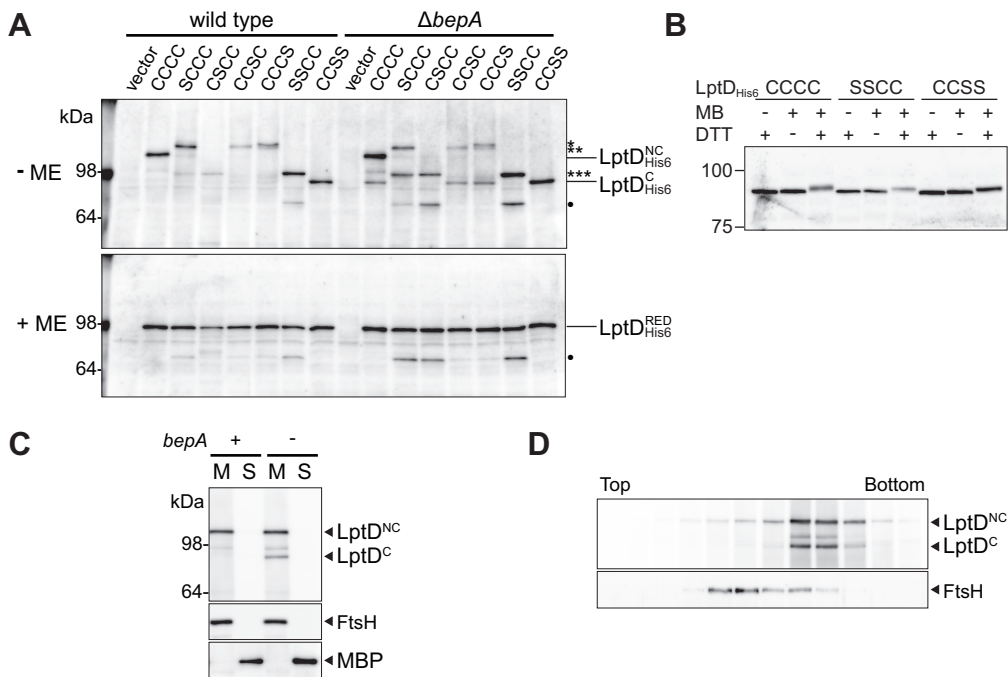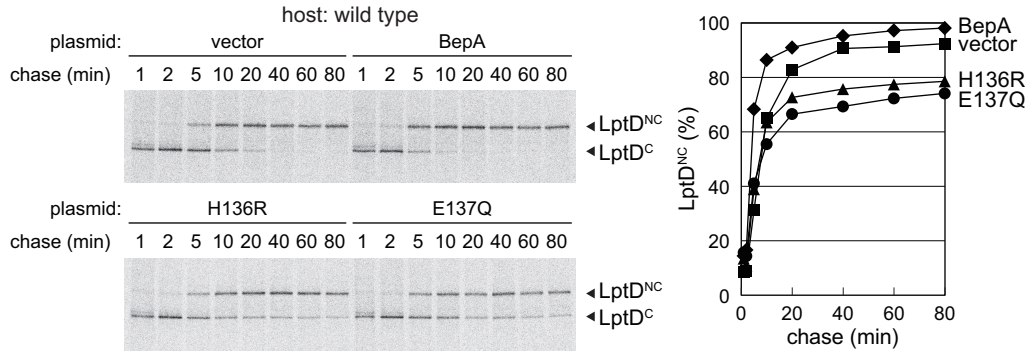
Fig. 3
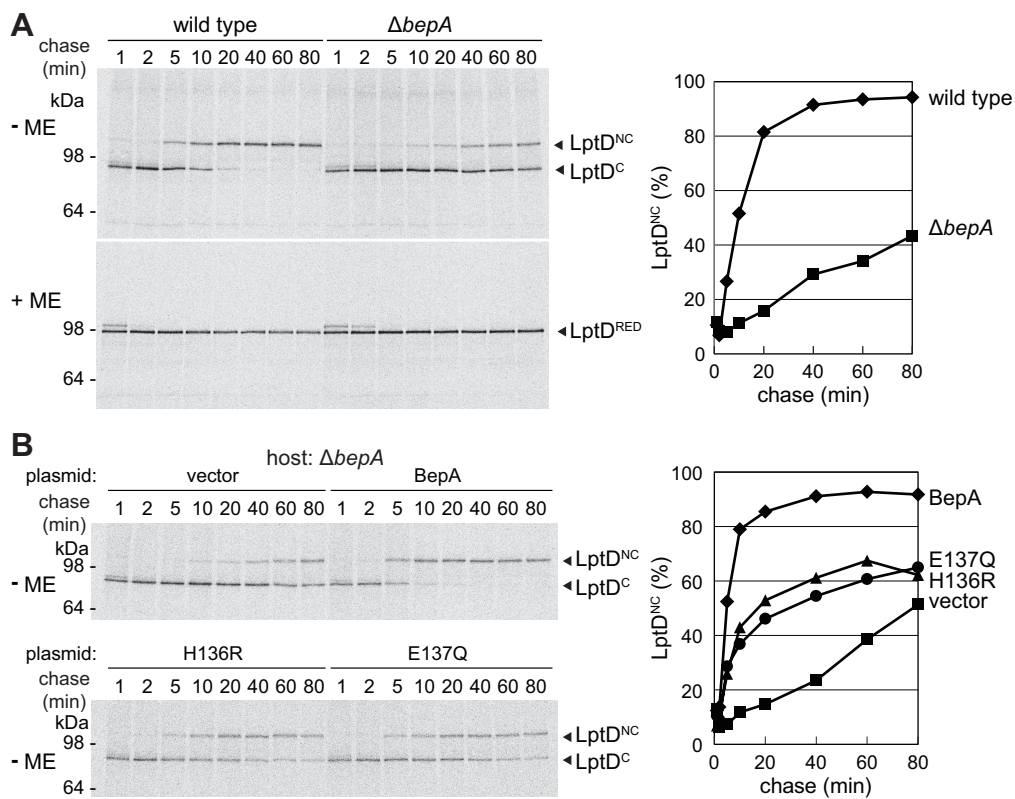
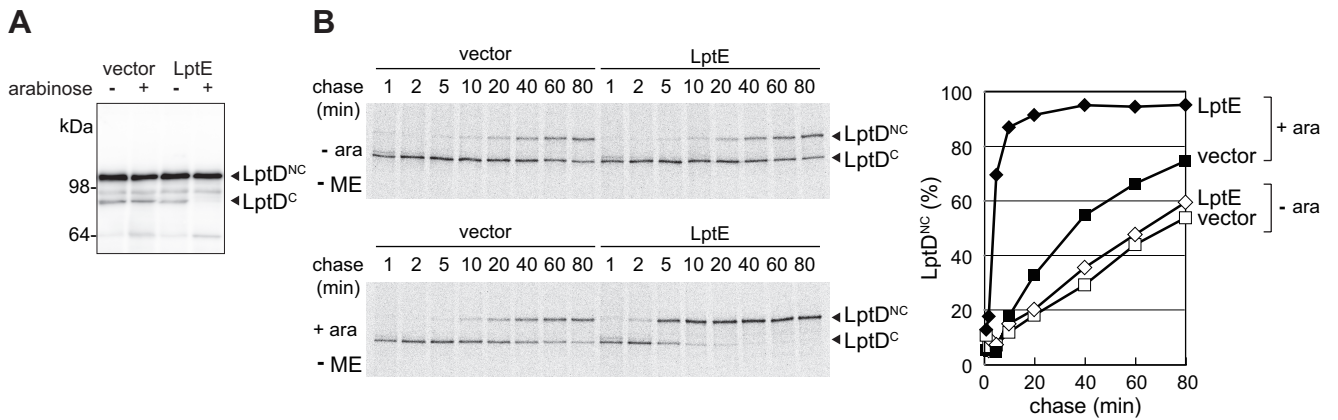Fig. 4

Fig. 5
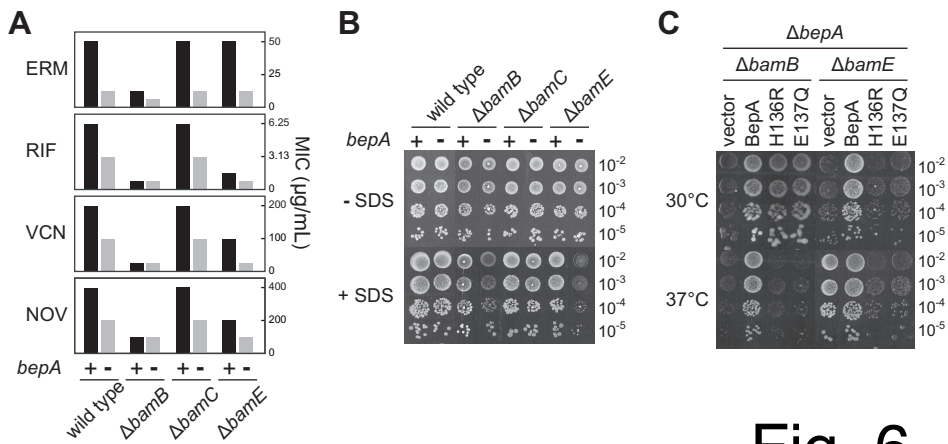
Fig. 6
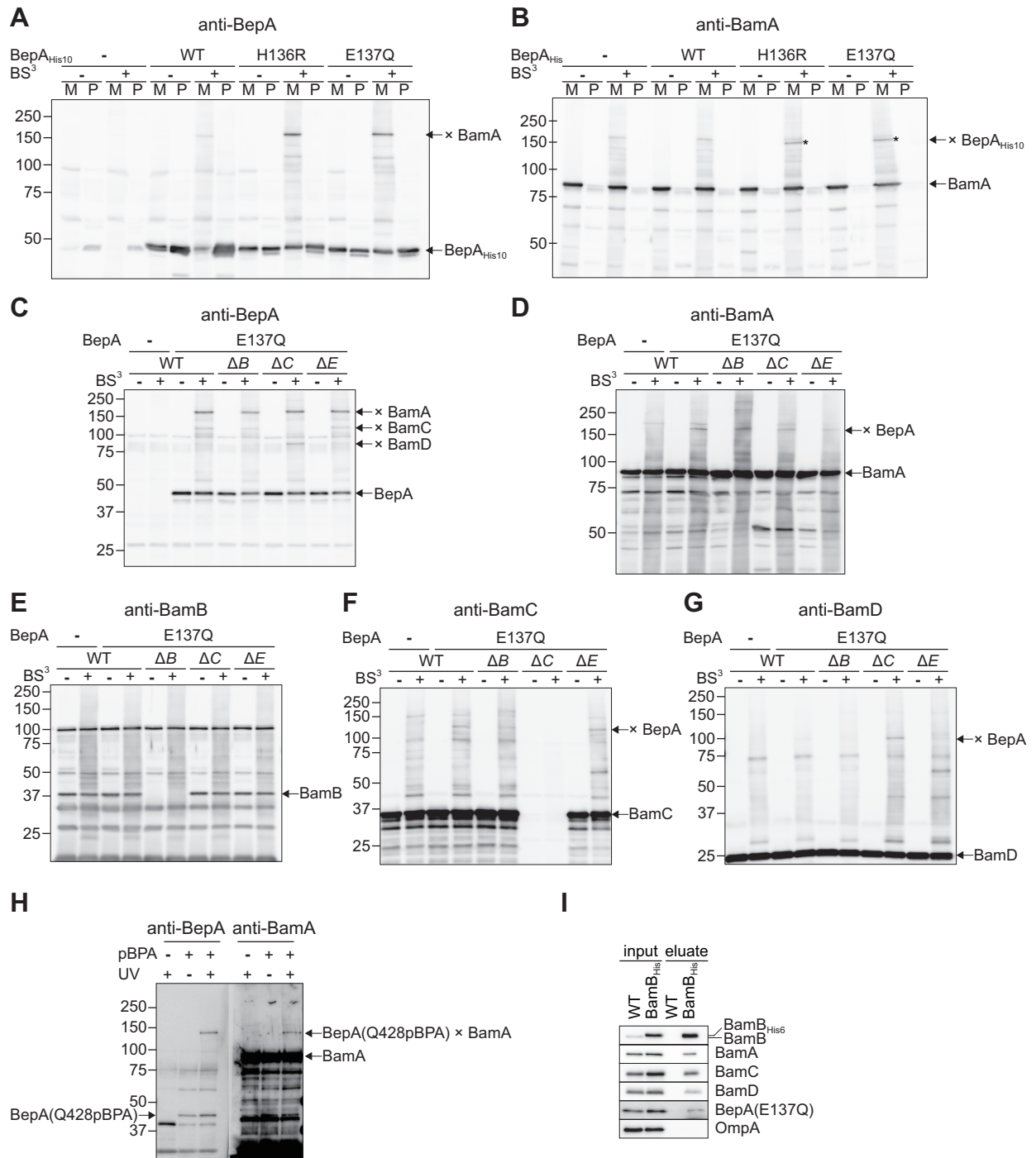
Fig. 7
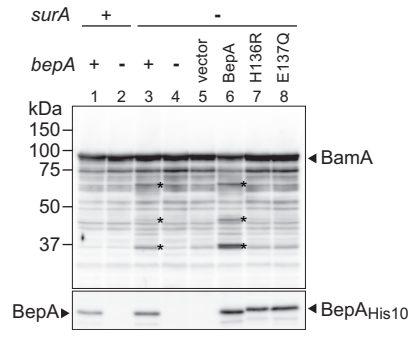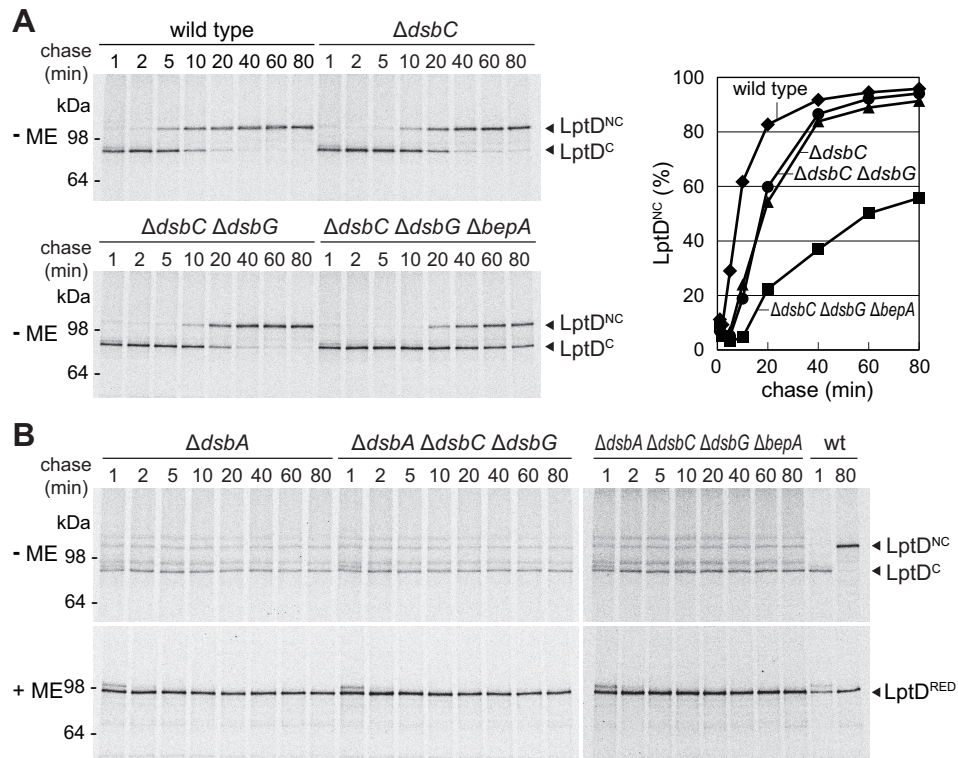
Fig. 8
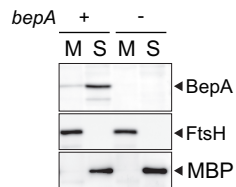

Fig. 9

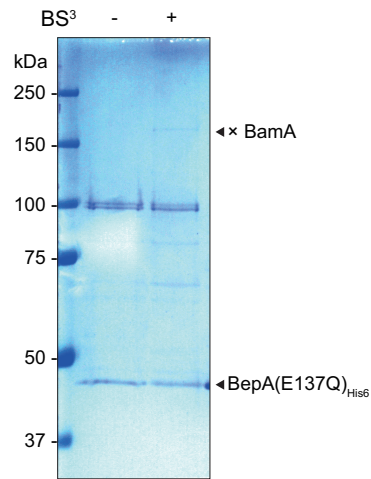Fig. S1

Fig. S2

Fig. S3

Fig. S4

Fig. S5

Fig. S6

Fig. S7

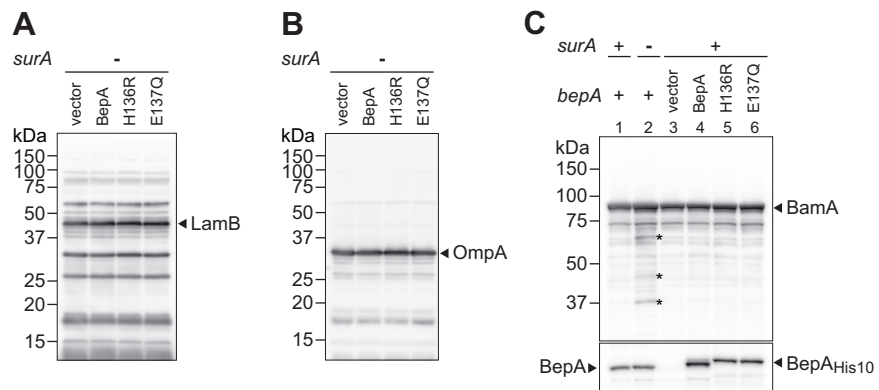Fig. S8

Table S1. List of ASKA plasmids that suppressed erythromycin sensitivity of the Δ*bepA* Δ*bamE* strain.

Plasmid[a]	Gene Product	Growth on SDS[b]	MIC of (μg/ml)			
			Erythromycin		Vancomycin	
			- IPTG	+ IPTG	- IPTG	+ IPTG
pTH-bepA-his$_{10}$	BepA	+	12.5	25	50	100
pCA24NΔNot	empty vector	-	6.25	3.13	25	25
fhuF	ferric iron reductase	+	25	12.5	25	50
mppA	murein tripeptide transporter	+	6.25	12.5	25	50
stfQ	predicted side tail fibre assembly protein	+	6.25	12.5	25	50
yaiU	conserved protein	+	6.25	12.5	25	50
ydfW	pseudogene, integrase fragment, Qin prophage	+	25	25	25	50
yeaH	conserved protein	+	6.25	12.5	25	25
ychP	predicted invasin	+	6.25	12.5	25	50
yneO	AidA homolog, autotransporter	+	6.25	12.5	25	25
ynjE	predicted thiosulfate sulfur transferase	+	6.25	12.5	25	50
appY	global transcription regulator	+	6.25	12.5	25	25
gadW	transcriptional activator of *gadA* and *gadBC*	+	6.25	12.5	25	50
soxS	DNA-binding transcriptional dual regulator	+	6.25	12.5	25	25
ydeO	transcriptional activator for *mdtEF*	+	6.25	25	25	50
rluE	23S rRNA U2457 pseudouridine synthase	+	6.25	12.5	25	25
lptE	LPS assembly OM complex	±	12.5	12.5	50	50
pagP	palmitoyl transferase for Lipid A	±	6.25	12.5	25	50
ybiI	DksA-type zinc finger protein	±	6.25	6.25	25	25
bcsC	cellulose synthase subunit	±	6.25	12.5	25	25
rrmJ	23S rRNA U2552 ribose 2'-O-methyltransferase	±	6.25	12.5	12.5	25
rplO	50S ribosomal subunit protein L15	-	6.25	6.25	25	25
rpsM	30S ribosomal subunit protein S13	-	6.25	6.25	25	25
ykgO	predicted ribosomal protein	-	6.25	6.25	25	25
marA	transcriptional activator of multiple antibiotic resistance	-	6.25	6.25	12.5	6.25
yaiT	conserved protein	-	6.25	12.5	25	50
yhfG	predicted protein	-	6.25	6.25	12.5	25

+, normal growth; ±, weak growth; −, no growth.

[a]Cloned genes in ASKA plasmids are shown.

[b]Growth phenotype on L agar containing 0.5% SDS is shown.

Table S2. Strains used in this study.

E. coli strains	Genotype	Reference
AD16	Δ*pro-lac thi* [F' *lacI*^q ZM15 *Y*⁺ *pro*⁺]	1
SN56	AD16 Δ*bepA*	This study
SN147	AD16 Δ*bamB*::*tet*	This study
SN150	AD16 Δ*bamB*::*tet* Δ*bepA*	This study
SN305	AD16 Δ*surA*::*kan*	This study
SN259	AD16 Δ*surA*::*kan* Δ*bepA*	This study
SN531	AD16 Δ*bamC*::*kan*	This study
SN533	AD16 Δ*bamC*::*kan* Δ*bepA*	This study
SN535	AD16 Δ*bamE*::*kan*	This study
SN537	AD16 Δ*bamE*::*kan* Δ*bepA*	This study
SN547	AD16 Δ*dsbA*::*kan*	This study
SN548	AD16 Δ*dsbA*::*kan* Δ*bepA*	This study
SN807	AD16 Δ*dsbC*	This study
SN773	AD16 Δ*dsbC* Δ*bepA*	This study
SN834	AD16 Δ*dsbC* Δ*dsbG*	This study
SN835	AD16 Δ*dsbC* Δ*dsbG* Δ*bepA*	This study
SN836	AD16 Δ*dsbA*::*kan* Δ*dsbC* Δ*dsbG*	This study
SN838	AD16 Δ*dsbA*::*kan* Δ*dsbC* Δ*dsbG* Δ*bepA*	This study
MC4100	*araD*139 Δ(*argF-lac*)*U*169 *rpsL*150 *relA*1 *flbB*5301	2
SN896	MC4100 Δ*bepA*	This study
SN909	MC4100 Δ*bamB*::*tet* Δ*bepA*	This study
SN910	MC4100 Δ*bamC*::*kan* Δ*bepA*	This study
SN911	MC4100 Δ*bamE*::*kan* Δ*bepA*	This study
AM604	MC4100 *ara*⁺	3
GC187	AM604 Δ*lptE2*::*kan* Δ(λ_{att}-*lom*)::*bla-P_{ara}lptE*(atg)-*araC*	Gift from T. Silhavy
SN1145	GC187 Km^S	This study
SN1159	SN1145 Δ*bepA*::*kan*	This study
SN1194	SN1145 Δ*bepA*	This study
KRX	Δ*pro-lac thi* [F' *traD*36 Δ*ompP lacI*^q ZM15 *pro*⁺] Δ*ompT endA*1 *recA*1 *gyrA*96 *hsdR*17 e14⁻ *relA*1 *supE*44 Δ*rhaBAD*::T7 RNA polymerase	Promega

1. Kihara A, Akiyama Y, Ito K (1996) A protease complex in the *Escherichia coli* plasma membrane: HflKC (HflA) forms a complex with FtsH (HflB), regulating its proteolytic activity against SecY. *EMBO J* 15(22): 6122–6131.

2. Casadaban MJ (1976) Transposition and fusion of the *lac* genes to selected promoters in *Escherichia coli* using bacteriophage lambda and Mu. *J Mol Biol* 104(3): 541-555.

3. Wu T, et al. (2006) Identification of a protein complex that assembles lipopolysaccharide in the outer membrane of *Escherichia coli*. *Proc Natl Acad Sci USA* 103(31): 11754-11759.

Table S3. Plasmids used in this study.

Plasmids	Description	Reference
pCA24NΔNot	Expression vector for ASKA clones; $P_{T5\text{-}lac}$ *cat*	This study
pCP20	pSC101 derivative; *Rep*(Ts) *bla cat* λcI857 λP_R *FLP*$^+$	1
pUC18	Expression vector; P_{lac} *bla*	2
pUC-bepA	pUC18 derivative encoding BepA	This study
pUC-bepA(H136R)	pUC18 derivative encoding BepA(H136R)	This study
pUC-bepA(E137Q)	pUC18 derivative encoding BepA(E137Q)	This study
pUC-BepA(Q428Amber)	pUC18 derivative encoding BepA(Q428Amber)	This study
pUC-bepA-his$_6$	pUC18 derivative encoding BepA$_{His6}$	This study
pUC-bepA-his$_{10}$	pUC18 derivative encoding BepA$_{His10}$	This study
pUC-bepA(H136R)-his$_{10}$	pUC18 derivative encoding BepA(H136R)$_{His10}$	This study
pUC-bepA(E137Q)-his$_{10}$	pUC18 derivative encoding BepA(E137Q)$_{His10}$	This study
pTTQ18	Expression vector; P_{tac} *bla*	3
pTTQ-bepA-his$_6$	pTTQ18 derivative encoding BepA$_{His6}$	This study
pTTQ-bepA(E137Q)-his$_6$	pTTQ18 derivative encoding BepA(E137Q)$_{His6}$	This study
pTH18cr	Expression vector; P_{lac} *cat*	4
pTH-bepA-his$_{10}$	pTH18cr derivative encoding BepA$_{His10}$	This study
pTH-bepA(H136R)-his$_{10}$	pTH18cr derivative encoding BepA(H136R)$_{His10}$	This study
pTH-bepA(E137Q)-his$_{10}$	pTH18cr derivative encoding BepA(E137Q)$_{His10}$	This study
pCDFDuet-1	Expression vector; P_{T7} *aadA*	Novagen
pCDF-bepA-his$_{10}$	pCDFDuet-1 derivative encoding BepA$_{His10}$	This study
pCDF-bepA(E137Q)-his$_{10}$	pCDFDuet-1 derivative encoding BepA(E137Q)$_{His10}$	This study
pEVOL-pBpF	p15A derivative encoding an evolved *M. jannaschii* aminoacyl-tRNA synthetase/suppressor tRNA pair for incorporation of pBPA at the amber site	5
pMAN885EH	Expression vector, P_{BAD} *cat*	6
pMAN-lptD-his$_6$	pMAN885EH derivative encoding LptD$_{His}$	This study
pMAN-lptD(C31S)-his$_6$	pMAN885EH derivative encoding LptD(SCCC)$_{His6}$	This study
pMAN-lptD(C173S)-his$_6$	pMAN885EH derivative encoding LptD(CSCC)$_{His6}$	This study
pMAN-lptD(C724S)-his$_6$	pMAN885EH derivative encoding LptD(CCSC)$_{His6}$	This study
pMAN-lptD(C725S)-his$_6$	pMAN885EH derivative encoding LptD(CCCS)$_{His6}$	This study
pMAN-lptD(C31S/C173S)-his$_6$	pMAN885EH derivative encoding LptD(SSCC)$_{His6}$	This study
pMAN-lptD(C724S/C725S)-his$_6$	pMAN885EH derivative encoding LptD(CCSS)$_{His6}$	This study
pMAN-lptE	pMAN885EH derivative encoding LptE	This study
pMAN-bamB-his$_6$	pMAN885EH derivative encoding BamB$_{His6}$	This study

1. Cherepanov PP, Wackernagel W (1995) Gene disruption in *Escherichia coli*: TcR and KmR cassettes with the option of Flp-catalyzed excision of the antibiotic-resistance determinant. Gene 158(1):9–14.

2. Yanisch-Perron C, Vieira J, Messing J (1985) Improved M13 phage cloning vectors and host strains: nucleotide sequences of the M13mp18 and pUC19 vectors. Gene 33(1):103–119.

3. Stark MJ (1987) Multicopy expression vectors carrying the lac repressor gene for regulated high-level expression of genes in *Escherichia coli*. Gene 51(2-3):255–267.

4. Hashimoto-Gotoh T, et al. (2000) A set of temperature sensitive-replication/-segregation and temperature resistant plasmid vectors with different copy numbers and in an isogenic background (chloramphenicol, kanamycin, *lacZ, repA, par, polA*). Gene 241(1):185–191.

5. Young TS, Ahmad I, Yin JA, Schultz PG (2010) An enhanced system for unnatural amino acid mutagenesis in *E. coli.* J Mol Biol 395(2):361–374.

6. Yakushi T, Tajima T, Matsuyama S, Tokuda H (1997) Lethality of the covalent linkage between mislocalized major outer membrane lipoprotein and the peptidoglycan of *Escherichia coli.* J Bacteriol 179(9):2857–2862.

Table S4. Primers used in this study.

Name	Sequence[a] (5' - 3')
yfgC-1	GATGAATTCCAGAAATACAGGATAGAG
yfgC-2	GGGGTACCTAATGATGATGATGATGATGCTCGAGCATCTTGGTATAAGGCTTAAAG
yfgC-3	ATGAATTCCAGGCAGTTGAAAAAAAACC
yfgC-4	CATGCCATGGTCAGGCAGTTGAAAAAAAACCTGG
M13 Primer M4	GTTTTCCCAGTCACGAC
yfgC-his10-1	CATCATCATCATTAAGTACCCG
yfgC-his10-2	ATGATGATGATGATGCTCG
yfgC_PstI-2	TTACATCTTGGTATAAGGCTTAAAGCGTTCCTGCA
yfgC_H136R	CTGGCTTCAGTTATGGCGCGCGAAATCTCCCACGTCACC
yfgC_H136R-r	GGTGACGTGGGAGATTTCGCGCGCCATAACTGAAGCCAG
yfgC_E137X	GGCTTCAGTTATGGCGCACYAGATCTCCCACGTCACCCAACG
yfgC_E137X-r	CGTTGGGTGACGTGGGAGATCTRGTGCGCCATAACTGAAGCC
TPR4-2	GCTAAATAACCGCGATTAGGAGCTGGCTGCGCG
TPR4-2-r	CGCGCAGCCAGCTCCTAATCGCGGTTATTTAGC
lptE-1	GATGAATTCTGGTCGTTGGCTAAGCGC
lptE-2	CAATTCAAGCTTCATTGAGCTGCGCGCGG
lptD-1	AACGTTACCGATGATGGAAC
lptD-2	CAATTCTCTAGATTAGTGATGGTGATGGTGATGCTCCAAAGTGTTTTGATACGGCAG
lptD_C31S	GCCGACCTCGCCTCACAGTCAATGTTGGGCGTGCCAAGC
lptD_C31S-r	GCTTGGCACGCCCAACATTGACTGTGAGGCGAGGTCGGC
lptD_C173S	CGGTAGCTTTACCTCCTCACTGCCGGGTTCTGACACCTG
lptD_C173S-r	CAGGTGTCAGAACCCGGCAGTGAGGAGGTAAAGCTACCG
lptD_C724S	GCAATACAGCTCCTCATGCTATGCAATTCGC
lptD_C724S-r	GCGAATTGCATAGCATGAGGAGCTGTATTGC
lptD_C725S	GTGCAATACAGCTCCTGCTCATATGCAATTCGCGTCGGTTAC
lptD_C725S-r	GTAACCGACGCGAATTGCATATGAGCAGGAGCTGTATTGCAC
lptD_C724S/C725S	GTGCAATACAGCTCCTCATCATATGCAATTCGCGTCGGTTAC
lptD_C724S/C725S-r	GTAACCGACGCGAATTGCATATGATGAGGAGCTGTATTGCAC
yfgL-1	GATGAATTCGGAGGTTTAAATTTATGCAATTGCGTAAATTACTGC
yfgL-2	CAATTCAAGCTTAGTGATGGTGATGGTGATGCTCCAGACGTGTAATAGAGTACACGGTTC

[a]The following IUB codes are used to indicate base mixtures: Y= C+T; R=A+G